

Predictive Study by Molecular Modeling To Promote Specific Probes of Glutamate Receptors, Using Methylated Cyclic Glutamic Acid Derivatives (*trans*- and *cis*-ACPD). Comparison with Specific Agonists

Nathalie Evrard-Todeschi,[†] Josyane Gharbi-Benarous,^{†,‡} Valéry Larue,^{†,§} and Jean-Pierre Girault^{*,†}

Laboratoire de Chimie et Biochimie Pharmacologiques et Toxicologiques (URA 400 CNRS),
Université René Descartes—Paris 5, 45 Rue des Saint-Pères, 75270 Paris Cedex 06, France, and
UFR Chimie, Université Denis Diderot—Paris 7, 2 Place Jussieu, 75251 Paris Cedex 05, France

Received January 2, 1998

Two classes of glutamate receptors (metabotropic and ionotropic) and their subclasses (groups I–III and *N*-methyl-D-aspartic acid (NMDA), kainic acid (KA)), respectively, are characterized by the binding of a L-glutamate moiety in a specific conformation. The conformations may be grouped by the two backbone torsion angles, χ_1 [α -CO₂[−]–C(2)–C(3)–C(4)] and χ_2 [⁺NC(2)–C(3)–C(4)– γ -CO₂[−]] and by the two characteristic distances between the potentially active functional groups, α -N⁺– γ -CO₂[−] (d_1) and α -CO₂[−]– γ -CO₂[−] (d_2). The conformational preferences of 2,3,4-methyl (**a** and **b**)-*cis* and *trans*-1-aminocyclopentane-1,3-dicarboxylate are discussed in the light of the physical features known for specific metabotropic (groups I–II) and specific ionotropic (NMDA, KA) agonists, respectively. The spatial orientation of the perceived functional groups was elucidated in cyclic derivatives which contain an embedded L-glutamate moiety in a partially restricted conformation (relative to the C(2)–C(3)–C(4) bond) using a combination of NMR experimental results and mechanics and dynamics calculations. One important conclusion of the study is that a single glutamate receptor is privileged for each theoretical model considered by molecular dynamics. This study showed clearly what would be the conformational preferences of cyclic glutamate derivatives following the geometrical isomerism of the methyl group.

INTRODUCTION

Glutamic acid is a major excitatory amino acid and neurotransmitter in the central nervous system.^{1,2} It mediates fast synaptic transmission in synaptic plasticity phenomena involved in brain development, learning, and memory.³ It has some role in neurodegenerative disorders such as epilepsy, plasticity, and Huntington's disease.⁴

Glutamate receptors have been classified as metabotropic (seven putative transmembrane domains, G-proteins coupled)^{5,6} or ionotropic (four putative transmembrane domains per subunit, ligand-gated channels). The ionotropic receptors are further subdivided into the receptors for *N*-methyl-D-aspartic acid (NMDA), (aminohydroxy)-5-methyl-4-isoxazol propionate (AMPA), and kainic acid (KA).^{7,8}

Recent molecular cloning studies on the metabotropic receptors have revealed the existence of at least eight different subtypes of mGluRs, termed mGluR1 to mGluR8.^{7,9–11} The eight mGluRs were classified into three groups:^{10,12} group I (mGluR1 and mGluR5) activated by *trans*-1-aminocyclopentane-1,3-dicarboxylate (1*S*,3*R*-*trans*-ACPD) and quisqualate (QUIS); group II (mGluR2 and mGluR3) activated by (1*S*,3*R*)-*trans*-ACPD and α -(carboxycyclopropyl)glycine (2*S*,3*S*,4*S*-L-CCG-I);^{13,14} group III (all the other mGluRs) selectively activated by L-AP4.^{12,15}

It is generally admitted that L-glutamic acid binds to the protein via its three ionizable groups, namely, α -amino and

α - and γ -carboxylates through hydrogen bondings¹⁶ or electrostatic interactions. L-Glutamic acid, a flexible molecule, displays different bioactive conformations; i.e., each receptor subtype would require a particular conformation of glutamate for its selective activation.¹⁷ As the acyclic molecule, glutamate can adopt nine *staggered* (and *eclipsed*) conformers resulting from rotation about C(2)–C(3) and C(3)–C(4) bonds (Figure 1) and, thus, is capable of fitting the different types of receptors.⁷ One method determining structure–activity relationships is to produce rigid analogues of glutamic acid. The introduction of conformationally restricted analogues of natural amino acids in substrates or inhibitors has proved helpful for studies of the geometry of binding sites.¹⁷

In previous studies by NMR and molecular modeling,^{18–22} cyclic and methylated glutamate analogues adopt several conformations which mimic the conformations of glutamic acid. These conformations, corresponding to a different spatial disposition of the three active groups, are defined by the two distances d_1 (α -NH₃⁺– γ -CO₂[−]) and d_2 (α -CO₂[−]– γ -CO₂[−]) (Figure 2). Two groups are considered to have an electrostatic interaction if their distance is less than (or equal to) 4 Å. Two families (**F_I** and **F_{II}**) were characterized by a d_1 distance shorter than d_2 : $d_1(\text{min})$ ($d_1 \ll d_2$) and $d_2(\text{max})$ ($d_1 < d_2$). Conversely, two other families (**F_{III}** and **F_{IV}**) were characterized by a d_2 distance shorter than d_1 : $d_1(\text{max})$ ($d_2 < d_1$) and $d_2(\text{min})$ ($d_2 \ll d_1$). Four other families (**F_R**–**F_{IV}**) with the same d_1 , d_2 distances will only differ in the sign of alkyl chain torsion angles χ_1 [α -CO–C(1)–C(2)–C(3)] and χ_2 [C(1)–C(2)–C(3)– γ -CO₂[−]] (Figure 3).

[†] Université René Descartes—Paris.

[‡] Université Denis Diderot—Paris.

[§] Present address: Laboratoire CSSB (UFR SMBH), Université Bobigny-Paris 13, 74 Rue Marcel Cachin, 93017 Bobigny, France.

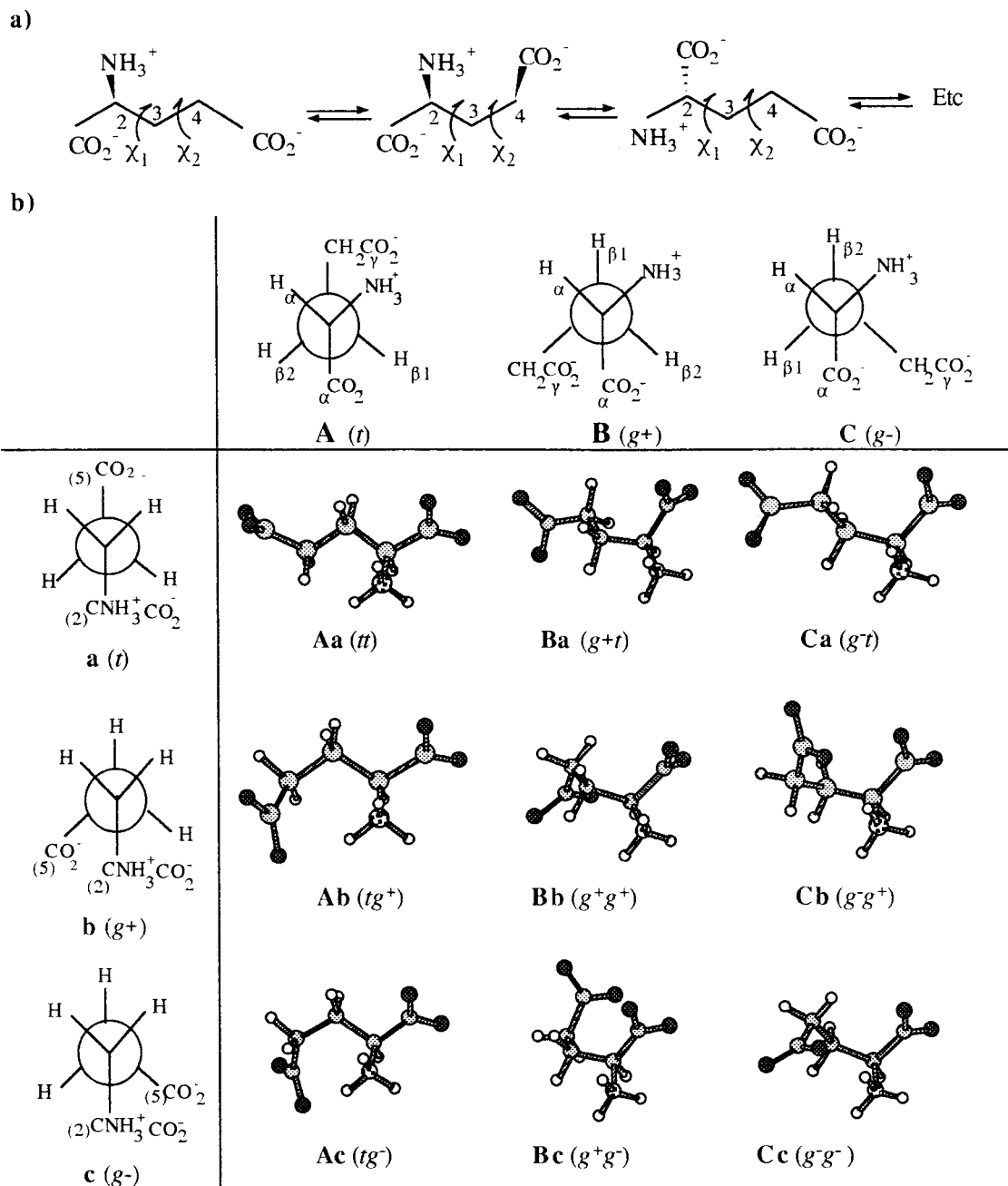


Figure 1. (a) Conformations of L-Glutamic acid around neutral pH; (b) Newmann projections for the three staggered rotamers "A, B, C" relative to the torsion angle χ_1 (C2–C3) and "a, b, c" relative to the χ_2 one (C3–C4) (t = anti and g = gauche). The nine conformations (Aa; Ab; Ac; Ba; Bb; Bc; Ca; Cb; Cc) of L-glutamic acid at pH 7.

Conformationally restricted analogues, cyclic and methylated glutamate, have been tested for some biological properties in comparison to glutamic acid (Figure 4). Cyclic glutamate analogues contain an embedded L-glutamate moiety, exhibiting a partially restricted rotation around (χ_1) and/or (χ_2) bonds. Indeed selective binding of these conformationally restricted analogues implies that glutamate may bind to each receptor in a distinct conformation.

Cyclic (ACPD, LCCG, and kainic acid) and methylated glutamate analogues (4E, 4T, and 4M) represent conformationally restricted analogues, but they retain some flexibility and therefore multiple conformers are likely to be populated in solution.^{18,19,22,23} The two ACPD isomers have been shown to be rather flexible, and they adopt envelope conformations which mimic the four conformational families (F_I–F_{IV}).¹⁸

There are still needs for more selective and potent drugs acting on ionotropic and metabotropic glutamate receptors that could help define the specific physiological roles of the different subtypes. One possible approach is to introduce steric hydrophobe groups on already characterized effectors. The aim of this paper is to lock the four possible conformations (F_I–F_{IV}) in completely rigid ACPD analogues by the introduction of a methyl in a different position (-2, -3, and -4) and configuration (a and b) for *cis*-ACPD or C5C (Figure 5a) and *trans*-ACPD or C5T (Figure 5b), in order to favor one bound conformational family. We have undertaken a predictive molecular dynamics (MD) study, to avoid the synthesis in a first step, of a battery of various ligands to obtain new conformationally constrained cyclic analogues of glutamic acid. The molecular modeling calculations have been performed under conditions similar to protocols undertaken for

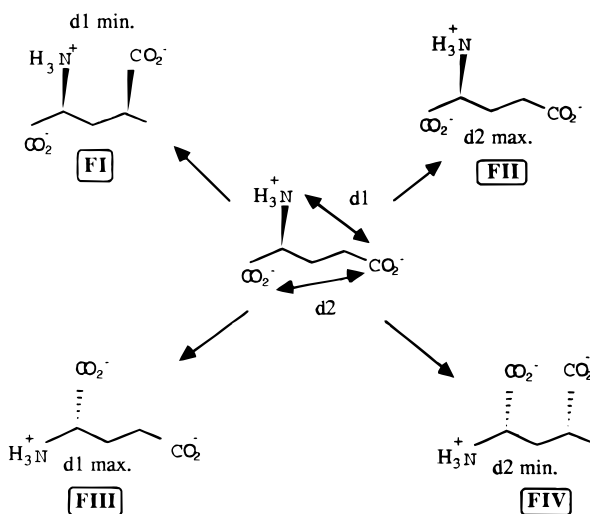


Figure 2. Representation of the four conformational families I–IV according to their characteristic distances $d_{1(\alpha\text{-NH}_3^+ - \gamma\text{-CO}_2^-)}$, $d_{2(\alpha\text{-CO}_2^- - \gamma\text{-CO}_2^-)}$.

corresponding ACPD analogues. Indeed, a good agreement observed between the MD approach and NMR results for ACPD molecules has encouraged us to develop this predictive molecular modeling study in order to determine the conformational families of the various methyl-ACPD isomers, with the protocol which seems to be appropriate. Different experiments were carried out, and thus, from these preliminary results, the synthesis and pharmacological activities of these new conformationally constrained cyclic analogues of glutamic acid will be tentatively deduced.

RESULTS AND DISCUSSION

A conformational search on the molecules whose ionized functional groups are $\gamma\text{-CO}_2^-$, $\alpha\text{-CO}_2^-$, and $\alpha\text{-NH}_3^+$ was performed by NMR (study at physiological pH) and MD. However, the receptor may be an acceptor or donor of protons. Hence, a number of structural features defined by the relative positions of the charged heteroatoms and the position of the hydrocarbon backbone can affect binding affinities. Thus, MD studies were performed on corresponding protonated or nonprotonated species, so as not to neglect protonation effects which will induce particular conformations.

Making use of the relevant structures generated by MD, the experiments provide useful information on the conformational behavior of aqueous ACPD derivatives using experimental values for the vicinal homo- and heteronuclear coupling constants, the pH dependence of coupling constants, and chemical shift data. For these compounds bearing a five-membered ring, particular problems arise due to ring strain; i.e., the strain in the molecule arises essentially from bond opposition and is partly relieved by puckered conformations. Particular effects on some coupling constants are expected. These points will be examined with caution. As a result, this extensive conformational study of ACPD isomers shall provide the basis for further molecular modeling and NMR studies of ACPD analogues or aminocyclopentanecarboxylic acid derivatives. Present study on ACPD is used to postulate a hypothesis about the conformational requirement of metabotropic (groups I–II) and ionotropic (NMDA, KA) glutamate receptors that it was interesting to strengthen and

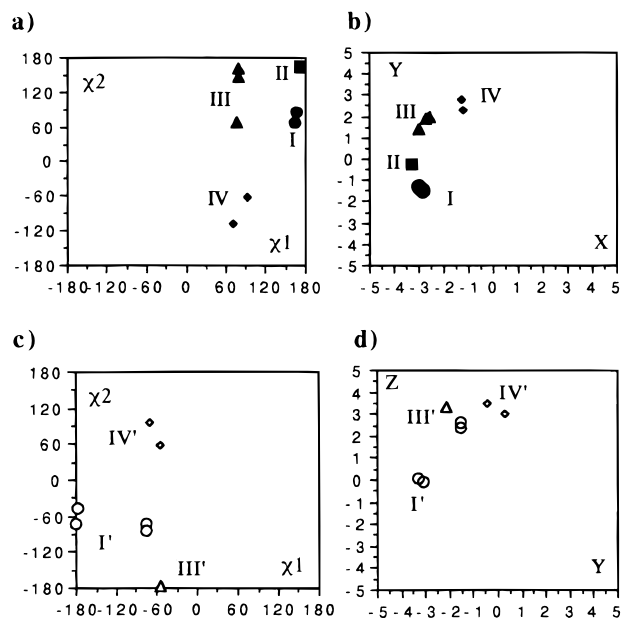
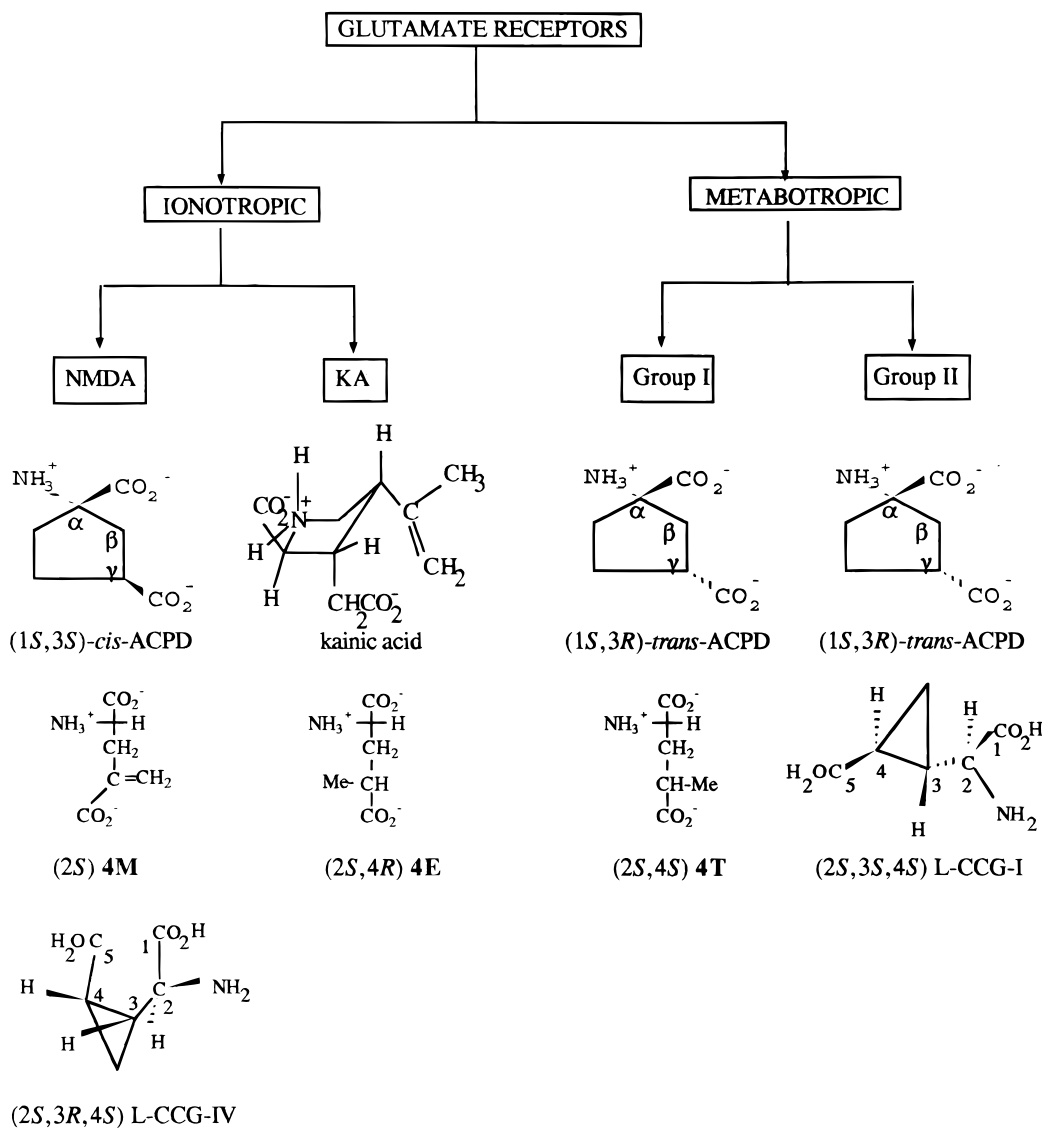


Figure 3. Symbols: ●, I; ■, II; ▲, III; ◆, IV; ○, I'; △, III'; ◇, IV'. The different conformational families I–IV and I'–IV' identified from the NMR and MD data of glutamate analogues are represented in a diagram according to the physical features of the potentially active functional groups: (a) the repartition of alkyl chain torsion angles χ_1 , χ_2 ; (b) the coordinates X, Y; (c) the repartition of alkyl chain torsion angles χ_1 , χ_2 ; (d) the coordinates X, Z of characteristic functional atoms $\alpha\text{-N}$, $\alpha\text{-C}$, $\gamma\text{-C}$.

to develop with methyl-ACPD derivatives. This extension is valid as the preliminary study was based on experimental homo- and heteronuclear coupling constant values and on calculations for which solvent and charges were considered.

First Part: Conformational Analysis of the *cis*- and *trans*-ACPD. These derivatives display some flexibility.¹⁸ In cyclopentane the angle of maximum puckering rotates without substantial change in potential energy. However, the presence of the three substituents will give rise to an induced potential energy barrier opposing free pseudorotation. The consequence of “limited” pseudorotation and a description of conformations was developed. In the present article, we propose an accurate description of rings in cyclopentyl analogues and the correlated conformations of the potentially active functional groups, $\alpha\text{-NH}_3^+$ and α - and $\gamma\text{-CO}_2^-$. The methodology presented illustrates the usefulness of molecular modeling in elucidating possible solution conformations and in exploring fully the conformational space of these compounds and NMR data in revealing that approximate solution structures can be estimated. NMR parameters reflect the virtual conformation, and at the same time the structural information of the different conformations generated by MD are of great benefit in predicting the conformation in solution. Thus, this study might allow us to shed light on the resulting conformation of ACPD analogues in aqueous solution. NMR experiments and computational investigation were undertaken in water in order to elucidate the conformational characteristics in a biological-type environment.

In cyclopentane, the two flexible forms, *envelope E* and *half-chair T* conformers are extremes of symmetry in the pseudorotational circuit of cyclopentane: 10 envelope and 10 half-chair forms interconvert by this process (Figure 6). In cyclopentane the angle of maximum puckering rotates



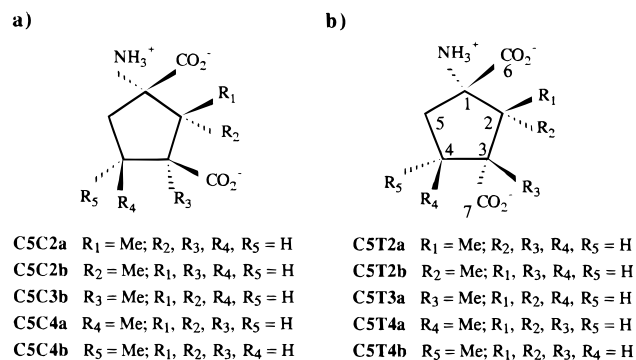


Figure 5. Structures of cyclopentane-derived analogues of glutamic acid studied at pH 7 (isomers α -S represented, zwitterions), *cis*-C5 (C5C) and *trans*-C5 (C5T) substituted by a methyl in position-2 (C5C2a, C5C2b and C5T2a, C5T2b), position-3 (C5C3b and C5T3a), and position-4 (C5C4a, C5C4b and C5T4a, C5T4b). The a face of the cyclopentane ring is that which contains the carboxyl group in position 1; CH₃ noted a or b according to the geometrical isomerism of the methyl (CH₃a and NH₃⁺ *trans*; CH₃b and NH₃⁺ *cis*).

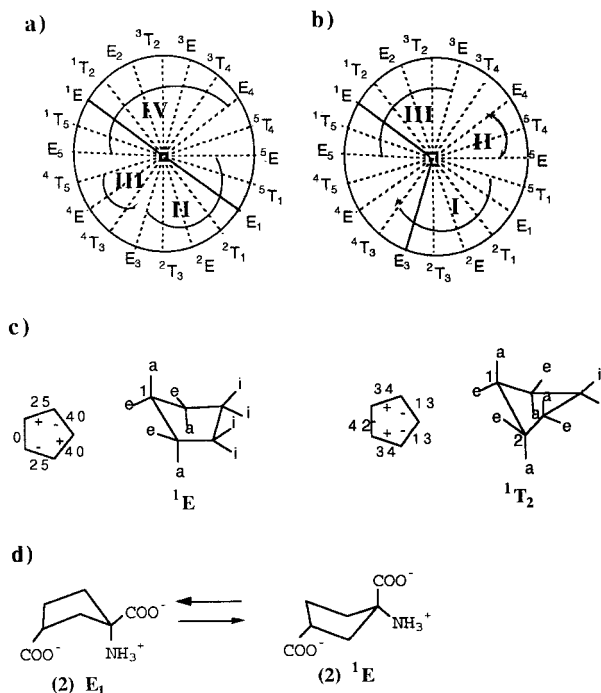


Figure 6. (a) Pseudorotational pathway of cyclopentane ring for *cis*-C5 (C5C) and (b) *trans*-C5 (C5T). Each external point of dotted radials in the circle represents a specific E form or T conformations. Heavy arrows indicate the corresponding family type. (c) Considered conformations for cyclopentane. The forms, envelope E and half-chair or twist T are represented in perspective drawing, as well as in the conventional formula indicating the approximate value of the torsion angles and their sign and with the following types of exocyclic bonds: equatorial (e), axial (a), and the so-called isoclinical (i) bonds. The former has four carbons in the same plane; in contrast, the half-chair has three coplanar carbon atoms, one above and one below (¹T₂); (d) conformations envelope E for C5T at pH 7, conformational equilibrium between the structure ¹E and another envelope E₁ when the out-of-plane carbon C-1 is pushed down.

calculated values (Table 1) for conformation ²E, E₁, E₃, ⁴E, or E₅ (Figure 7) but are not in good agreement with the calculated values for conformation ¹E, ³E, or ⁵E.

The *trans*-ACPD or C5T (Figure 5b) may be found as a mixture of one sterically favored conformation with the

3-CO₂⁻ group equatorial and another conformer (isoclinical H(3a), axial 3-CO₂⁻, being very probably stabilized by an electrostatic interaction (analogous to a hydrogen bond) between the 1-ammonium (α -NH₃⁺) and the 3-carboxylate group (γ -CO₂⁻). H(3a) is in an isoclinical position, more weakly coupled with its neighboring *trans* protons H(2b) and H(4b) and found nearly eclipsing protons H(2a) and H(4a) (large coupling). This inversion is observed for the calculated values (Table 2) of E₁ and E₃ conformations, while the data ³J_{(3a)C(1)} = 3.5 Hz and ³J_{C(5)H(3a)} = 2.5 Hz, include a large participation of conformer E₁ (³J_{H(3)C(1)} = 4.5 Hz and ³J_{H(3)C(5)} = 2.0 Hz) (Table 2). The experimental values are not in good agreement with the calculated values (Table 2) for conformation ³E or ⁴E.

It is thus concluded, from NMR data, that C5C exists in solution as one major ²E conformer and C5T as one major E₁. These preferred conformations are the sterically and the electrostatically favored ones, very likely stabilized by the interactions between the α -amino and γ -carboxylate groups and by the least interactions between the cyclopentane ring and the α - and γ -carboxylate groups. Other minor conformation(s) could also participate in solution, such as E₁, E₃, ⁴E, and E₅ for *cis*-ACPD or E₃, E₂, ⁵E, and ¹E for *trans*-ACPD, respectively. All of these conclusions will be further tested using molecular dynamics experiments.

(B) Molecular Modeling. The aims of the molecular modeling are as follows: (i) to select a set of conformations to be considered in the conformational analysis of NMR data (the computed torsion angles then form a basis for determination of the experimental conformer populations *via* Karplus equations); (ii) to evaluate the theoretical conformer populations and compare them with the experimental ones (this can be achieved *via* Maxwell-Boltzmann statistics (Table 3) or by MD calculations (Tables 4 and 5); we will show below that only MD simulations give interesting results).

Whatever the aim, we have to choose how to describe the intra- and intermolecular interactions. A good procedure for choosing the appropriate force field to identify the experimentally determined conformation as the lowest energy structure is to fit the parameters of the interaction function to results (potential or field) of ab initio quantum calculations on a small molecular cluster. The alternative is to fit the force field parameters on experimental data such as, in our case, NMR data. We have chosen this second way, and in order to develop an adequate molecular model of the two analogues, we have tested the ability of two force fields, CVFF²⁸ and TRIPOS²⁹ (as implemented in BIOSYM and SYBYL programs, respectively), to reproduce the NMR experimental data.

The lowest energy conformations found by Maxwell-Boltzmann statistics or by MD with the CVFF force field using $\epsilon_r = 5$ was in excellent agreement with the experimental structures. This result has suggested to us that the Biosym CVFF force field was an adequate tool for modeling the ACPD compounds, and it shall be utilized in molecular modeling studies of the other structural analogues. We used the CVFF force field from Dauber-Osguthorpe²⁸ in which cross-terms represent the coupling of the deformations of internal coordinates and describe the coupling between adjacent bonds. These terms are required to reproduce accurately experimental vibrational frequencies and therefore

Table 1. Torsion Angles and Calculated^a Coupling Constants (³J, Hz) Computed for the *Envelopes* Generated by MD [Homonuclear (¹H,¹H) and Heteronuclear (¹³C,¹H) NMR Coupling Constants in D₂O (Hz, Error 0.3 Hz) Used in the Conformational Analysis of **C5C**; H Noted **a** or **b** According to the Geometrical Isomerism of the Proton (**Ha** and NH₃⁺ *trans*; **Hb** and NH₃⁺ *cis*)]

rotamer	theoretical torsion angles/deg (³ J/Hz)								NMR ³ J/Hz	MD	
	² E	^E ₃	⁵ E	^E ₁	⁴ E	^E ₅	¹ E	³ E		³ J ^b /Hz	³ J ^c /Hz
3b,2a	-171.4 (12.1)	-167.9 (12.0)	-124.5 (5.3)	-161.9 (11.4)	-151.7 (10.1)	-125.5 (5.5)	-94.6 (1.7)	-74.7 (1.9)	12.0	11.5	7.8
3b,2b	-53.7 (4.1)	-51.9 (4.4)	-10.2 (9.5)	-44.5 (5.6)	-36.9 (6.6)	-10.8 (9.5)	-26.9 (8.0)	41.9 (5.9)	6.5	4.8	6.0
3b,4a	149.8 (9.8)	172.4 (12.2)	94.3 (1.7)	135.8 (7.5)	169.5 (12.1)	156.6 (10.8)	130.4 (6.4)	75.4 (1.9)	10.0	9.5	8.5
3b,4b	30.6 (7.5)	51.4 (4.5)	-25.6 (8.1)	16.4 (9.1)	48.2 (5.0)	35.8 (6.8)	11.4 (9.5)	-45.1 (5.4)	8.5	7.5	5.5
4a,5a	8.0 (9.6)	-38.5 (6.5)	41.9 (5.9)	-21.9 (8.6)	-46.2 (5.3)	-46.1 (5.3)	-33.5 (7.2)	32.2 (7.3)	12.0	9	5.9
4a,5b	-106.7 (2.7)	-152.7 (10.3)	-76.0 (1.8)	-94.1 (1.7)	-162.3 (11.4)	-163.8 (11.6)	-151.1 (10.0)	-83.1 (1.6)	7.0	3.1	7.6
4b,5a	125.2 (5.5)	91.2 (1.6)	161.2 (11.3)	139.6 (8.2)	74.4 (2.0)	73.6 (1.9)	84 (1.6)	151.9 (10.1)	3.5	5.5	4.3
4b,5b	10.5 (9.5)	-33 (7.2)	43.3 (5.7)	23.7 (8.3)	-41.8 (5.9)	-44.1 (5.6)	-33.6 (7.0)	36.6 (6.6)	8.0	8.9	6.1
ΣΔJ _{HH} (MD/NMR)										13.5	18.6
3b-H, 1-C	75.0 (0.7)	70.2 (1.0)	116.3 (1.8)	97.1 (0.6)	92.4 (0.5)	-120.6 (2.3)	143.3 (4.6)	161.8 (6.2)	<1	0.8	1.8
3b-H, 5-C	-92.9 (0.6)	-74.1 (0.8)	-144.3 (4.7)	-123.0 (2.3)	-78.8 (0.6)	-94.0 (0.6)	115.7 (1.8)	-163.3 (6.4)	<1	0.8	2.0
ΣΔJ _{HH} (MD/NMR)										0.4	1.8

^a The coupling constants values ³J_{HH} and ³J_{HC} were calculated by using Karplus-type equations: ³J = A cos² φ + B cos φ + C with different coefficients in the homonuclear case (³J_{HH}) A = 9.5, B = -1.3, and C = 1.6 and in the heteronuclear case (³J_{HC}) A = 5.7, B = -0.6, and C = 0.5.

^b Protocol 1 (with ε = 5 and the protonated or nonprotonated species favored at pH 3 (α-CO₂H, γ-CO₂⁻, and α-NH₃⁺): 77% ²E + 3% ^E₃ + 13% ^E₁ + 6% ^E₅). For each *i*th conformational microstate, the average coupling constant can be computed from ³J_{HH} = ΣP_{*i*}J_{*i*}(HH) and ³J_{HC} = ΣP_{*i*}J_{*i*}(HC) [³J_{3b,2a} = 77% J_{3b,2a}(²E) + 3% J_{3b,2a}(^E₃) + 13% J_{3b,2a}(^E₁) + 6% J_{3b,2a}(^E₅) = 7.8 Hz (J_{obs} = 11.5)]. ^c Protocol 2 (solvation box with ε = 1 and the protonated or nonprotonated species favored at pH 7 (α- and γ-CO₂⁻ and α-NH₃⁺): 20% ^E₃ + 8% ⁵E + 7% ^E₁ + 35% ⁴E + 6% ^E₅ + 3% ¹E + 16% ³E).

the dynamic properties of molecules. A Morse function was used to describe the stretching of bonds.

Particular attention had to be given in the modeling of electrostatic interactions which are calculated in the force field by a Coulombic expression. A widely used method for mimicking the solvent screening effect is to use a distance-dependent relative permittivity ε = *r*, leading to an *r*² dependence of the Coulombic energy.³⁰ In previous studies,³¹ to model implicitly the solvent effect, we adjusted the relative permittivity to a value between 1 and 78 (ε = 5, ε = 4*r*), corresponding to the interactions in aqueous solution. It is sometimes better to mimic the solvent with explicit modeling of water. So, we constructed solvation boxes around the charged end groups of the molecules containing several water molecules by using periodic boundary conditions.³²

In addition to getting the best agreement between theoretical (MD) and experimental (NMR) data, the purpose of this work is also to give some insight into the water exchange on the three ions. Simulations were carried out on systems *cis*- and *trans*-ACPD containing one positive ammonium ion and two negative carboxylate ones and a reasonable number of 48 water molecules. Because of the presence of the cyclopentyl group on the same carbon that bears the ammonium and carboxylate groups, the hydration of the molecule is mainly governed by electrostatic and steric factors to represent the water–water intermolecular interactions, the ion–water interaction, and the ligand-field effects.

Of course, the molecular modeling can only implicitly take the pH into account by working on the protonated or

nonprotonated species favored at pH 3 (α-CO₂⁻, γ-CO₂H, and α-NH₃⁺) and pH 7 (α-CO₂⁻, γ-CO₂⁻, and α-NH₃⁺).

(1) Molecular Mechanics. The first step in the modeling consisted of minimizing the structure previously constructed, to find a local energy minimum on the potential energy hypersurface of the molecule. Calculations were performed according to several algorithms commonly used in molecular mechanics for choosing descent directions, namely, steepest descent and conjugate gradient methods. A protocol was conceived that would rapidly give results in conformational studies, avoiding the introduction of explicit water molecules (ε = 5 and ε = 4*r*). The results are summarized in Table 3.

The relative population of the *i*th conformational state, *P_i*, with energy, *E_i*, is dictated by the Boltzmann distribution,

$$P_i = \exp(-E_i/kT) / \sum \exp(-E_j/kT)$$

We have calculated the population of different conformations using Maxwell–Boltzmann statistics.

Note that for *cis*-ACPD (**C5C**), most of the calculations (ε = 5) lead to the good major conformers ²E (pH 3 and 7), in some agreement with NMR results (²E or ^E₃), just as using an explicit solvent description (Table 3). For *trans*-ACPD (**C5T**), the Boltzmann probabilities with the introduction of explicit water molecules included in CVFF force field and with ε = 5 at pH 3 lead to the major “¹E” and the minor “³E” conformations, while the results obtained with ε = 5 at pH 7 give the predominant NMR “^E₁” conformation (Table 3).

The ability of the CVFF force field to reproduce the experimental NMR-determined major conformations of **C5C**

Table 2. Torsion Angles and Calculated^a Coupling Constants (³J, Hz) Computed for the *Envelopes* Generated by Molecular Modeling [Homomuclear (¹H,¹H) and Heteronuclear (¹³C,¹H) NMR Coupling Constants in D₂O (Hz, error 0.3 Hz) Used in the Conformational Analysis of **C5T**; H Noted **a** or **b** According to the Geometrical Isomerism of the Proton (**Ha** and NH₃⁺ *trans*; **Hb** and NH₃⁺ *cis*)]

rotamer	theoretical torsion angles/deg (³ J/Hz)							NMR ³ J/Hz	MD	
	E ₁	E ₄	E ₃	E ₅	E ₂	E ₆	E ₇		³ J ^b /Hz	³ J ^c /Hz
3a,2a	-24.1 (8.3)	49.8 (4.7)	-33.1 (7.2)	8.4 (9.6)	52.7 (4.2)	44.4 (5.6)	41.0 (6.Q)	8.5	7.4	5.9
3a,2b	91.5 (1.6)	165.8 (11.8)	82.4 (1.6)	122.6 (5.1)	169.3 (12.0)	162.7 (11.5)	158.9 (11.1)	4.5	5.6	7.7
3a,4a	-4.6 (9.5)	-51.5 (4.5)	29.6 (7.6)	-32.8 (7.2)	-51 (4.5)	-17.9 (8.9)	-12.2 (9.4)	8.0	8.3	6.0
3a,4b	-123.4 (5.1)	-172.8 (12.3)	-88.7 (1.6)	-152.7 (10.3)	-171.5 (12.1)	-137.1 (7.6)	-131.5 (6.5)	5.0	7.0	8.7
4a,5a	26.0 (8.1)	36.3 (6.8)	-23.4 (8.4)	41.9 (5.9)	32.2 (7.3)	-22.2 (8.6)	-27.1 (8.0)	7.5	7.5	6.9
4a,5b	-90.7 (1.6)	-79.3 (1.7)	-138.2 (7.8)	-76.0 (01.8)	-83.1 (1.6)	-138.4 (7.8)	-143.7 (8.9)	4	3.5	2.6
4b,5a	143.3 (8.7)	156.2 (10.7)	93.9 (1.7)	161.2 (11.3)	151.9 (10.1)	95.3 (1.8)	90.6 (1.6)	8.5	7.3	8.2
4b,5b	26.7 (8.0)	40.6 (6.0)	-20.9 (8.7)	43.3 (5.7)	36.6 (6.6)	-21.0 (8.7)	-25.9 (8.1)	7.0	7.4	6.6
ΣΔJ _{HH} (MD/NMR)									6.6	14.2
3a-H, 1-C	-141.6 (4.5)	-74.4 (0.8)	-150.8 (5.3)	-110.9 (1.5)	-70.8 (0.9)	-78.8 (0.6)	-82.7 (0.5)	3.5	1.9	3.2
3a-H, 5-C	116.6 (2.0)	68.9 (1.0)	146.9 (5.0)	88.6 (0.5)	70.0 (0.9)	101.8 (0.9)	107.0 (1.2)	2.5	1.5	1.5
ΣΔJ _{HH} (MD/NMR)									2.6	1.3

^a The coupling constants values ³J_{HH} and ³J_{HC} were calculated by using Karplus-type equations: ³J = A cos² φ + B cos φ + C with different coefficients in the homonuclear case, (³J_{HH}) A = 9.5, B = -1.3, and C = 1.6, and in the heteronuclear case, (³J_{HC}) A = 5.7, B = -0.6, and C = 0.5. ^b Protocol 1 (with ε = 5 and the protonated or nonprotonated species favored at pH 3 (α-CO₂⁻, γ-CO₂H, and α-NH₃⁺): 44% **E**₁ + 3% **E**₃ + 18% **E**₅ + 12% **E**₂ + 23% **E**₆). For each *i*th conformational microstate, the average coupling constant can be computed from ³J_{HH} = ΣP_{*i*}³J_{HH(*i*)} and ³J_{HC} = ΣP_{*i*}³J_{HC(*i*)} [³J_{3a,2a} = 44% ³J_{3a,2a}(**E**₁) + 3% ³J_{3a,2a}(**E**₃) + 18% ³J_{3a,2a}(**E**₅) + 12% ³J_{3a,2a}(**E**₂) + 23% ³J_{3a,2a}(**E**₆) = 7.4 Hz (*J*_{obs} = 8.5)]. ^c Protocol 2 (solvation box with ε = 1 and the protonated or nonprotonated species favored at pH 7 (α- and γ-CO₂⁻ and α-NH₃⁺): 18% **E**₁ + 11% **E**₃ + 3% **E**₅ + 17% **E**₄ + 40% **E**₂ + 2% **E**₆ + 3% **E**₇).

(**E**₂) and **C5T** (**E**₁) suggest that CVFF force field is an adequate tool for modeling these compounds.

The Boltzmann probabilities did not generate the approximate ratios of minimum-energy conformations available respectively for **C5C** and **C5T** in aqueous solution. For these charged and flexible molecules, it is obvious that MD studies may have to be used to get more reasonable statistical participation of every structure to improve the NMR result.

(2) Molecular Dynamics. The second step of the conformational sampling procedure involved recording the MD trajectories (including the charge distributions in CVFF force field). By solving the equations of motion for a system of atoms, MD has an advantage in that it is not restricted to harmonic motion about a single minimum but allows molecules to cross energy barriers and explore other stable conformations. To simulate the molecular motions in solution, different protocols of MD have been used. In MD calculations, the empirical force field methods are able to produce a collection of structures that span all the accessible conformational space of the molecule. In order to find suitable parameters (solvent and electrostatic term, number of water molecules, times, temperature) for simulation of these specific molecules, we varied them systematically and performed 120 simulations (Tables 4 and 5).

We ran experiments starting from each one of the ten possible conformations (*envelope E*) of the two compounds (**C5C** and **C5T**) to compare their energies and to determine their frequency in the interconversion. In addition, we carried out simulations starting from each one of the ten conformers of **C5C** and **C5T**, in various protonation states, with different values of ε and in aqueous environment to

get the best agreement between theoretical (MD) and experimental (NMR) data. These experiments lead to a statistical evaluation of the different conformations which contribute to the results obtained by NMR analysis. The ability of a force field to reproduce the experimental NMR-determined conformations suggests that no modification would be made in this appropriate force field for modeling the compounds.

The important electrostatic (the α-NH₃⁺ and the γ-CO₂⁻ groups) and steric (cyclopentyl ring and intermediate eclipsed forms) contributions lead to a very good stabilization of some conformations and hinder an interconversion of the corresponding rotamers since the energetic barriers are too high. Consequently, in a first study, conformational analysis of these amino acids began with the simple assumption of one dominating conformation, **E**₂ in *cis*-ACPD and **E**₁ in *trans*-ACPD. Most of the time, if MD experiments is performed from the ten different starting structures with implicitly taking account of the solvent (ε = 5) and with CVFF force field, they yield the major conformer. An ambiguity remains about the other low-energy conformers. Each structure is further refined by putting the molecules (**C5C** and **C5T**) in a solvent box of H₂O. As we will see below, the MD trajectories with hydration boxes and with CVFF force field were not the most efficient in finding ACPD conformations in agreement with NMR data (Table 5).

(a) cis-ACPD. Protocols were carried out with CVFF force field using different values of the dielectric constant (ε = 5 or ε = 4*r*). We can observe (Table 4, Figure 7a) that, with ε = 5 and the protonated or nonprotonated species favored at pH 3 (α-CO₂⁻, γ-CO₂H, and α-NH₃⁺), the

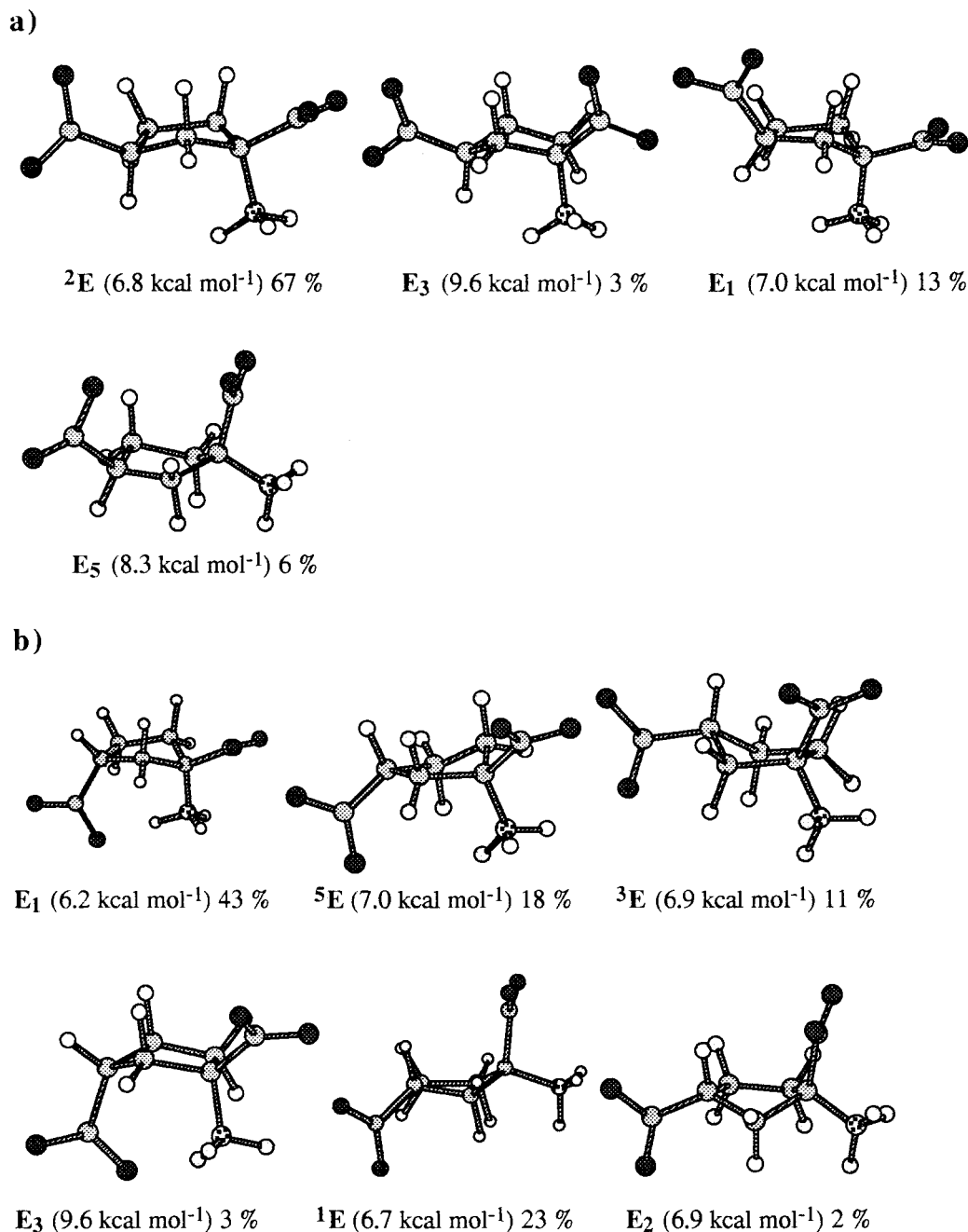


Figure 7. (a) Stable structures generated by the protocol with a selected value of the relative permittivity ($\epsilon = 5$) for **C5C** and (b) achieved conformations for **C5T** by MD and only the forms, *envelope E* are represented. Potential energies of the corresponding C5 molecules: ${}^2\text{E}$ $E_{\text{pot.}} = -126.2$ (7.7) kcal mol $^{-1}$; ${}^2\text{T}_3$ $E_{\text{pot.}} = -126.0$ (7.8) kcal mol $^{-1}$; E_3 $E_{\text{pot.}} = -118.3$ (8.7) kcal mol $^{-1}$.

conformation ${}^2\text{E}$ was highly predominant (77%). Different experiments were carried out, and one minor NMR E_1 conformation was generated in the same proportion (10–15%), whereas in the water box, with the CVFF force field, the major conformation is now the ${}^4\text{E}$ one ($\sim 35\%$) while ${}^3\text{E}$ or E_3 conformations are also favored (16 and 20%, respectively). This result is not in good agreement with NMR data. The differences observed between MD and NMR results have discouraged us from developing this study in a solvation box filled with water molecules in order to improve the composition of the **C5C** derivative solution.

(b) *trans*-ACPD. Most of the simulations lead to a unique or a very highly favored conformation E_1 , whereas the experimental conformational mixture contains amounts of minor E_3 , E_2 , ${}^3\text{E}$, ${}^5\text{E}$, or ${}^1\text{E}$. Here also, as for *cis*-ACPD,

only the protocol with the CVFF force field and with the protonated or nonprotonated species ($\alpha\text{-CO}_2^-$, $\gamma\text{-CO}_2\text{H}$, and $\alpha\text{-NH}_3^+$) seems to be appropriate since the best agreement is observed with the experimental NMR-determined populations. Indeed, from the various averaging resulting from the MD approach, the set 44% E_1 + 23% ${}^1\text{E}$ + 18% ${}^5\text{E}$ + 12% ${}^3\text{E}$ + 3% E_3 presented good agreement with the populations of conformers obtained from NMR spectra (Table 4, Figure 7b).

The fit between MD and the experimental data also indicates that the conformational space was well-sampled^{33,34} and allows us to choose the best MD protocols for ACPD derivative molecules. The small difference is attributed to a slight variation of the minor conformers that affects the conformational averaging in solution.

Table 3. Energies (kcal mol⁻¹) and Boltzmann Probabilities (BP, %) of the *Envelope* Conformations for the Two Isomers (**C5C** and **C5T**) Obtained by Molecular Mechanics (ϵ the Dielectric Constant Used in the Force Field Equations; the Conformations Obtained by Molecular Mechanics Are Represented In Bold)

starting conformations	C5C						C5T									
	$\epsilon = 5^a$		$\epsilon = 5^b$		box ^c		$\epsilon = 5^a$		$\epsilon = 5^b$		box ^c					
	$E_{\text{pot.}}$		$E_{\text{pot.}}$		$E_{\text{pot.}}$		$E_{\text{pot.}}$		$E_{\text{pot.}}$		$E_{\text{pot.}}$					
	BP	BP	BP	BP	BP	BP	BP	BP	BP	BP	BP	BP				
¹ E	E₅	8.4	0	2E	5.0	100	1E	−649.5	1E	7.4	15	1E	6.1	0	1E	−601.1
² E	2E			2E			2E	−651.6	5E	7.1	25	E₁			2E	−648.7
³ E	2E			2E			2E	−659.6	5E			E₁			3E	−620.0
⁴ E	2E			2E			4E	−631.2	E₃	9.7	0	E₁			E3	−642.3
⁵ E	2E			2E			5E	−666.7	5E			E₁			E3	−655.4
E ₁	2E	7.0	100	2E			2E	−670.4	5E			E₁	1.5	100	E₁	−636.2
E ₂	2E			2E			5E	−648.7	1E	6.6	60	E₁			5E	−654.0
E ₃	2E			2E			4E	−644.4	E₃			E₁			E₁	−634.4
E ₄	2E			2E			E₁	−669.4	5E			E₁			5E	−643.2
E ₅	E₅	8.4		2E			E₅	−631.7	1E			E₁			1E	−659.5
																100

^a Protocol 1 (with $\epsilon = 5$ and the protonated or nonprotonated species favored at pH 3 (α -CO₂⁻, γ -CO₂H, and α -NH₃⁺). ^b Protocol 2 (with $\epsilon = 5$ and the protonated or nonprotonated species favored at pH 7 (α - and γ -CO₂⁻ and α -NH₃⁺). ^c Protocol 3 (Solvation box with $\epsilon = 1$ and the protonated or nonprotonated species favored at pH 7 (α - and γ -CO₂⁻, and α -NH₃⁺); the energies obtained are those of "molecule + 48 H₂O" systems.

Table 4. Simulations (20 ps) at 300 K for the Ten *Envelope* Conformations with $\epsilon = 5$ and the Protonated or Nonprotonated Species Favored at pH 3 (α -CO₂⁻, γ -CO₂H, and α -NH₃⁺) for **C5C** and **C5T** Isomers^a

C5C starting conformations										total freq	percentage	family	
¹ E	² E	³ E	⁴ E	⁵ E	E ₁	E ₂	E ₃	E ₄	E ₅				
¹ E											0	0	
² E	× (124)	× (165)	× (140)	× (160)	× (200)	× (160)	× (150)	× (141)	× (162)	× (142)	1544	77	F_{II}
³ E	× (1)		× (3)				× (2)				0	0	
⁴ E		× (18)									6	0	
⁵ E	× (49)	× (9)	× (50)	× (27)		× (13)	× (21)	× (29)	× (11)	× (54)	18	1	F_{II}
E ₁											263	13	F_{II}
E ₂		× (8)	× (2)	× (9)		× (13)	× (11)	× (4)	× (12)	× (3)	0	0	
E ₃								× (1)			62	3	F_{II}
E ₄	× (26)		× (5)	× (4)		× (14)	× (16)	× (25)	× (15)	× (1)	1	0	
E ₅											106	6	F_{IV}

C5T starting conformations										total freq	percentage	family	
¹ E	² E	³ E	⁴ E	⁵ E	E ₁	E ₂	E ₃	E ₄	E ₅				
¹ E	× (44)	× (46)	× (60)	× (62)	× (67)	× (53)		× (69)	× (8)	× (47)	456	23	F_{III}
² E	× (42)	× (5)	× (47)	× (31)	× (24)	× (9)		× (3)			3	0	
³ E								× (36)	× (2)	× (32)	228	11.5	F_{III}
⁴ E		× (9)	× (18)	× (1)	× (10)	× (22)		× (52)	× (189)	× (48)	0	0	
⁵ E	× (92)	× (105)	× (71)	× (93)	× (98)	× (114)	× (199)	× (37)		× (61)	349	17.5	F_{II}
E ₁	× (11)		× (4)	× (11)	× (1)	× (1)				× (4)	870	43.5	F_I
E ₂	× (8)	× (35)				× (1)	× (1)	× (3)	× (1)	× (8)	32	1.5	F_{III}
E ₃	× (1)			× (2)							57	3	F_I
E ₄	× (2)										3	0	
E ₅											2	0	

^a Each column represents one simulation; "×" indicates that conformation was found, and the frequency is given in parentheses. Frequency is the number of times each conformation is found.

The problem in using MD searching for ligand binding conformations, particularly if the ligands are ions or highly charged molecules, is to not neglect protonation sites that will induce particular conformations.

The coupling constants were calculated from the corresponding dihedral angles of each conformer generated by MD (Tables 1 and 2). Averaging is required to correctly predict the conformational properties like *J*-couplings. By using *P_i*, the fractional population for each *i*th conformational microstate, the average coupling constant can be computed from:

$${}^3J_{(\text{HH})} = \sum P_i {}^3J_{i(\text{HH})} \quad \text{and} \quad {}^3J_{(\text{HC})} = \sum P_i {}^3J_{i(\text{HC})}$$

Experimental values were compared to the calculated values

from the conformational equilibrium generated by the summed MD trajectories (Tables 4 and 5). The different experiments were analyzed, and we found good correlation (Tables 1 and 2) between the NMR coupling constants and those calculated from the conformational averaging obtained (Table 4) with $\epsilon = 5$ and the protonated or nonprotonated species (α -CO₂⁻, γ -CO₂H, and α -NH₃⁺): [77% ²E + 13% **E₁** + 6% **E₅** + 3% **E₃**] for **C5C**; [44% **E₁** + 23% ¹E + 18% ⁵E + 12% ³E + 3% **E₃**] for **C5T**. The $\sum \Delta(J_{\text{calc}} - J_{\text{exp}})$ evaluated from about ten coupling constants (*J_{H,H}* and *J_{C,H}*) lead to an average value ($\langle \Delta \rangle \pm 1$ Hz) which show without ambiguity that solution averaging is well-described in good agreement with the NMR data.

The experiments will provide useful information on the conformational behavior of aqueous glutamate analogues

Table 5. Simulations (200 ps) at 300 K for the Ten *Envelope* Conformations in the Solvation Box with $\epsilon = 1$ and the Protonated or Nonprotonated Species Favored at pH 7 (α - and γ -CO₂⁻ and α -NH₃⁺) for **C5C** and **C5T** Isomers^a

C5C starting conformations											total	percentage	family
¹ E	² E	³ E	⁴ E	⁵ E	E ₁	E ₂	E ₃	E ₄	E ₅	freq			
¹ E	× (100)	× (3)	× (5)	× (22)						27	3	F _{IV}	
² E		× (63)	× (63)	× (2)	× (6)	× (2)			× (6)	19	2	F _{II}	
³ E		× (63)	× (27)	× (25)	× (28)	× (49)	× (67)	× (67)	× (50)	163	16	F _{IV}	
⁴ E		× (1)	× (68)		× (1)	× (1)	× (6)			349	35	F _{III}	
⁵ E		× (18)		× (3)	× (22)	× (18)	× (2)	× (2)	× (8)	77	8	F _{II}	
E ₁			× (1)							73	7	F _{II}	
E ₂	× (39)			× (70)	× (42)	× (16)	× (23)	× (1)	× (13)	1	0		
E ₃			× (14)			× (1)		× (11)		204	20	F _{II}	
E ₄	× (3)				× (1)	× (13)	× (2)	× (19)	× (23)	26	3	F _{III}	
E ₅										61	6	F _{IV}	
C5T starting conformations											total	percentage	family
¹ E	² E	³ E	⁴ E	⁵ E	E ₁	E ₂	E ₃	E ₄	E ₅	freq			
¹ E	× (2)					× (6)	× (6)	× (3)		17	2	F _{III}	
² E	× (52)	× (12)		× (15)			× (1)			28	3	F _I	
³ E			× (4)		× (5)	× (67)	× (78)	× (40)	× (97)	401	40	F _{III}	
⁴ E	× (11)	× (1)	× (11)	× (1)				× (1)		1	0		
⁵ E	× (4)	× (83)		× (76)				× (6)		30	3	F _{II}	
E ₁	× (5)					(6)	× (6)		× (17)	186	18	F _I	
E ₂		× (4)		× (8)	× (95)		× (21)		× (25)	57	6	F _{III}	
E ₃	× (26)		× (85)			× (33)	(10)	× (2)		109	11	F _I	
E ₄								× (17)		171	17	F _{II}	
E ₅										0	0		

^a Each column represents one simulation; "×" indicates that conformation was found, and frequency is given in parentheses. Frequency is the number of times each conformation is found.

using experimental values for the vicinal homo- and hetero-nuclear coupling constants, pH and the temperature dependence of coupling constants, and chemical shift data and making use of theoretically calculated vicinal coupling constants on the relevant structures generated by MD. The methodology presented illustrates the usefulness of MD in elucidating possible solution conformations and NMR data in revealing that approximate solution structures can be estimated.

As three acidity functions are present in these compounds, the charges of the groups α -NH₃⁺, α -CO₂⁻, and γ -CO₂⁻ and their protonations depend on the pH of the solution, the preferred conformation may depend on these charges because of the electrostatic interactions or hydrogen bonding implied. At isoelectric pH (pH_i = 3), γ -carboxylate group is protonated and can provide a distal carboxylic acid which possesses a potential proton donor hydroxyl group. The conformational preferences were affected by the solvent environment due to the stabilization of the asymmetric charge distribution by interaction with the solvent. The free energy of interaction between three ions α -NH₃⁺, α -CO₂⁻, and γ -CO₂⁻ and a dipolar solvent varies with the charge on the ion. Minimization in a solvent box with the introduction of explicit water molecules reduce the electrostatic contribution. The most accurate way of including an environment is to explicitly include the solvent atoms themselves. This is, of course, more expensive computationally. The effective electrostatic interaction between two charged end groups of a molecule will be reduced as water molecules will arrange themselves so as to effectively screen the interaction. If the solvent molecules are explicitly included in the simulation, then this effect will already be taken into account, and the dielectric constant assigned should be close to 1. We have constructed solvation boxes containing 48 water molecules using boundary conditions and MD experiments were carried

out at neutral pH on the zwitterionic molecules with ionized functional groups γ -CO₂⁻, α -CO₂⁻, and α -NH₃⁺. One notices that, from for **C5T** starting structures, the E₁ conformation stabilized by the electrostatic interaction between γ -CO₂⁻ and α -NH₃⁺ in spite of hydration is not predominantly generated. This result not in agreement with **C5T** NMR data may be explained since MD reveals that water molecules are located between the two charged groups. The distance between the two opposite charges is very small (≤ 3 Å), and water molecules should surround both charges at the same time rather than each charge separately. The less good correspondence for ACPD derivatives molecules indicates a difficult compromise between the steric contributions (cyclopentyl ring and intermediate eclipsed forms) and any intramolecular stabilizing forces and, thus, suggests a relative modification of the force field. So, if we reduce the electrostatic contribution on ACPD molecules by removing one formal charge (i.e. on the the γ -carboxylate group), we conceive a protocol at isoelectric pH with functional groups γ -CO₂H, α -CO₂⁻, and α -NH₃⁺ during 200 ps at 300 K ($\epsilon = 5$). The E₁ conformations are now favored, and the calculated populations of conformers are then in a better agreement with the NMR experimental data, for these isomers. This agreement probably arises because the calculations have included the hydration effects of the aqueous solvent.

The aim of the conformational preferences is to find all the thermally populated conformations of a molecule, i.e., the conformations with the lowest free energies, in order to provide important structural information on the properties of the molecule. The modeling procedure was used to generate the approximate ratios of low-energy conformers.

The practical methodologies employ molecular dynamics generating conformations and include experimental analysis to determine the 3-D structure from NMR data.

The advantage MD has in approaching thermodynamic equilibrium instead becomes a problem when searching for a particular high free energy conformation. For example, the conformation a molecule adopts after binding a receptor could be several kilocalories per mole higher in potential energy when calculated by itself than the energy of the global minimum. This will cause a problem if one tries to use MD searching for such receptor binding conformations, particularly if the ligands are ions or highly charged molecules which is likely to have a large influence on their structures. The receptor may be an acceptor or donor of protons. Hence, we have extended the NMR and the MD study in water at different pH values, so as not to neglect protonation effect which will induce particular conformations. It was interesting to examine the conformational changes induced by the electrostatic field generated by the different polarity of these molecules. If one examines the transformation of the molecules which occurred in the solvation box during the MD experiments (300 K with jumps to 600 K), one observes that the presence of water molecules favored during the trajectory some “less-staggered” rotamers which represent high-energy intermediates close to a particular transition state implied in the *envelope* conversion.

Second Part: Conformational Analysis of the Methylated-ACPD. As a continuation to obtain new conformationally constrained cyclic analogues of glutamic acid, in order to provide new and useful data for the elaboration of pharmacophores of ionotropic and metabotropic receptors, the predictive molecular dynamics study of the methylated cyclopentane ring (Figure 5) has been carried out with $\epsilon = 5$ and the protonated or nonprotonated species favored at pH 3 (α -CO₂⁻, γ -CO₂H, and α -NH₃⁺). Then, since good agreement is obtained for *cis* and *trans*-ACPD, nothing else was changed in the force field considering that it was well-fitted.

(A) Molecular Modeling. We performed computational chemical methods (molecular mechanics and molecular dynamics calculations), starting with the *envelope* structures of **C5C** and **C5T** for the simulation of 2,3,4 (**a** and **b**)-methyl-*cis*- and *trans*-ACPD (**C5C2a**, **C5C2b**; **C5C3b**; **C5C4a**, **C5C4b**, and **C5T2a**, **C5T2b**; **C5T3a**; **C5T4a**, **C5T4b**), respectively. Charges and atomic potentials were then redefined for the new molecules using the built-in algorithm of the program. The structures were minimized with “steepest descent” and “conjugate gradients” steps, until convergence. Electrostatic interactions are calculated in the force field²⁸ by a Coulombic expression. The final structures obtained after several such calculations were examined for the overall energetic favorability.

(1) Molecular Mechanics. The different conformations of the ten isomers are minimized by molecular mechanics (Table 6). All calculations are performed, using a relative permittivity (dielectric constant) $\epsilon = 5$. We have calculated the population of different conformations using Maxwell–Boltzmann’s statistics. The results are summarized in Table 6. We can observe that for each methylated analogue one major *envelope* conformation is obtained (**E**₁ for **C5C2a**, **C5C3b**, **C5C4b**, **C5T2b**; **E**₁ for **C5C2b**, **C5T2a**; **E**₃ for **C5C4a**, **C5T3a**, **C5T4b**; **E**₅ for **C5T4a**). According to the previous results obtained for the **C5C** and **C5T**, it is known that ranking the conformations only to their potential energies is misleading. The MD protocol that has been conceived

Table 6. Energies (kcal mol⁻¹) and Boltzmann Probabilities (BP, %) of the *Envelope* Conformations for the Different Isomers Obtained by Molecular Mechanics^a

starting conformations	C5C2a		C5C2b		C5C3b		C5C4a		C5C4b		C5T2a		C5T2b		C5T3a		C5T4a		C5T4b	
	<i>E</i> _{pot.}	BP	<i>E</i> _{pot.}	BP	<i>E</i> _{pot.}	BP	<i>E</i> _{pot.}	BP	<i>E</i> _{pot.}	BP	<i>E</i> _{pot.}	BP	<i>E</i> _{pot.}	BP	<i>E</i> _{pot.}	BP	<i>E</i> _{pot.}	BP	<i>E</i> _{pot.}	BP
E ₁	14.9	100	16.3	100	13.4	100	5.9	18	8.8	26	16.4	41	20.4	41	13.6	5	5.7	21	8.4	21
E ₂	E ₁		21.5		11.6	89	E ₃	82	8.4	52	18.4	2	16.7	2	E ₁	23	5.7	79	E ₃	79
E ₃	E ₁		13.6	100	13.7	3	E ₃	5.0	8.9	22	E ₁		19.5		12.7	10	4.9		E ₃	
E ₄	E ₁				13.5	4	E ₃				16.2	57	17.3		12.1	62	11.2		E ₃	
E ₅	E ₁				E ₁	89	E ₃				E ₁		E ₁		E ₃		5.7		E ₃	
E ₁	E ₁				E ₁		E ₃		11.9		E ₁		E ₁		E ₁		5.7		E ₁	13.9
E ₂	E ₁		16.3		E ₁		E ₃				E ₁		E ₂		E ₁		E ₂		E ₁	
E ₃	E ₁				E ₃		E ₃				E ₁		E ₃		E ₃		9.4		E ₃	8.7
E ₄	E ₁		13.6		E ₃		E ₃				E ₁		E ₁		E ₃		5.7		E ₄	
E ₅	E ₁		13.6		E ₁		E ₅				E ₁		E ₁		E ₁		E ₂		E ₄	

^a ϵ is the dielectric constant used in the force field equations. The conformations obtained by molecular mechanics with $\epsilon = 5$ and the protonated or nonprotonated species favored at pH 3 (α -CO₂⁻, γ -CO₂H, and α -NH₃⁺) are represented in bold type.

Table 7. Results of the MD Simulations Using a Protocol with $\epsilon = 5$ and the Protonated or Nonprotonated Species Favored at pH 3 (α -CO₂⁻, γ -CO₂H, and α -NH₃⁺)^a

family		C5T	C5T2a	C5T2b	C5T3	C5T4a	C5T4b	family		C5C	C5C2a	C5C2b	C5C3	C5C4a	C5C4b
FIII	¹ E	23	98		9		25	FIV	¹ E	10	60		16	1	30
FI	² E	11.5	2	1	7	5		FII	² E	67	38		30	4	
FIII	³ E							FIV	³ E		2			5	3
FI	⁴ E	17.5			5	79		FIII	⁴ E	1			1	1	
FII	⁵ E	43.5		72	44		3	FII	⁵ E	13		100	34	42	3
FI	E ₁	1.5		10		16		FII	E ₁						
FIII	E ₂	3		17	34		55	FIV	E ₂	3			17	28	50
FI	E ₃				1		17	FII	E ₃					19	
FII	E ₄							FIII	E ₄	6			2		14
FIII	E ₅							FIV	E ₅						
FI		46.5	—	90	78	—	58	FII		84	38	100	52	72	83
FII		17.5	—	—	6	79	17	FIII		—	—	—	—	24	3
FIII		36	100	10	16	21	25	FIV		16	62	—	48	4	14

^a Percentage of each *envelope* conformation generated with this protocol, starting from the ten *envelope* conformations of each isomer (for each isomer 2000 structures were examined).

with NMR data (on **C5C** and **C5T** analogues) can be used directly and rapidly for the conformational analysis of other charged methyl-ACPD molecules of a similarly limited size. A protocol avoiding the introduction of explicit water molecules is the preferred choice, and, in this case, the appropriate value of the relative permittivity is 5 with the protonated or nonprotonated species (α -CO₂⁻, γ -CO₂H, and α -NH₃⁺).

(2) Molecular Dynamics. For an exploration of the conformational space, after an equilibration period of 6 ps, the dynamics are run at 300 K. During a simulation a number of quantities, such as the potential and kinetic energies, are generally monitored to obtain a picture of the stability of the simulation.³² The stability of the different conformers has been tested by a 200 ps dynamics protocol at 300 K. The 200 ps trajectory is sampled every picosecond; the structures are then minimized by molecular mechanics and stored. We have run experiments starting from each one of the ten *envelope* conformations of the ten compounds to compare their energies and to determine their frequency in the interconversion. The results are summarized in Table 7. The major conformations obtained according this protocol ($\epsilon = 5$ and pH 3) are represented in Figures 8 and 9.

We have run dynamics from methyl-*cis*-C5-ACPD molecules (Figure 8, Table 7). The lowest-energy conformers **E₁** and **E₃** were stable when the methyl group is located on the *b* face of the cyclopentane ring which contains the 1-amino groups **C5C2b**, **C5C3b**, **C5C4b**, confirming 25% of the conformations obtained from **C5C**. The minor **C5C2a** structure, ²**E** achieved by MD, was predominant in **C5C** solution (~75%) according to NMR results. It should be noticed that, in these conformations, the three 1,3-carboxylate and -methyl groups are lying equatorial. Conversely, the major **C5C2a** structure, ¹**E** (1-CO₂⁻ axial and 3-CO₂⁻ isoclinal) such as the minor **C5C3b** structures, ¹**E** and ³**E** (1,3-CO₂⁻ axial and 1-NH₃⁺, Me isoclinal or equatorial) were hardly generated from **C5C** since they were probably destabilized by an overestimated electrostatic repulsion between the two 1,3-diaxial carboxylate groups. It was important to notice that these "folded" structures, ¹**E** and ³**E** would be now sterically stabilized by the equatorial orientation of the methyl group.

We have run dynamics from methyl-*trans*-C5-ACPD molecules (Figure 9, Table 7). When the methyl group is

located on the *a* face of the cyclopentane ring which contains the 1-carboxylate groups, the lower-energy **E₁** and **E₃** conformers were stable (~80%) only for the isomer **C5T3a**, confirming the NMR and MD results of the **C5T** (47%). In these two **E₁** and **E₃** conformations, the 3-methyl equatorial group increases the axial character of the 3-carboxylate group and favors a 1,3-diaxial electrostatic interaction between the 1-NH₃⁺ and 3-CO₂⁻ in an axial position. The preferred conformation of the **C5T2a** and **C5T4a** molecules is the sterically favored one (with three equatorial or isoclinal groups: 3-CO₂⁻, 1-NH₃⁺, and 2-CH₃ or 1,3-CO₂⁻ and 4-CH₃), respectively, ¹**E** and ⁵**E** showing either a large "W" between the 1-amino and the 3-carboxylate groups or between the 1-carboxylate and the 4-methyl groups. It is interesting to note that for the *trans*-isomers, **C5T2b** and **C5T4b**, with the methyl group located on the *b* face of the cyclopentane ring which contains the 1-amino and the 3-carboxylate groups, the steric interactions are predominant. Nevertheless, the lower-energy **E₁** and **E₃** conformers (~90–60%) are again privileged by the methyl equatorial group, 3-CO₂⁻ and 1-NH₃⁺ staying respectively in a folded position (axial) stabilized by the 1,3-electrostatic attraction.

In the two types of structures methyl-*cis*- and *trans*-C5 generated by MD, the methyl group always adopted an equatorial (or isoclinal) position, whatever the envelope conformation was.

Third Part: Similarity Analysis. The conformationally restricted analogues, cyclic (ACPD, LCCG, and kainic acid) and methylated (**4E**, **4T**, and **4M**) glutamate, have been tested for some biological properties in comparison to glutamic acid (Figure 4). The (1*R*,3*R*)-*cis*-ACPD or **C5C**, (2*S*,3*R*,4*S*)-L-CCG-IV, and the 4-methylene-L-glutamate (**4M**)³⁵ have been identified as potent agonists of the ionotropic NMDA receptor, while the [(2*S*,4*R*)-4-methylglutamic acid] (**4E**) was identified as having exceptional selectivity for the KA ionotropic receptor subtype³⁶ originally identified and characterized by its selective interaction with α -kainic acid. The (1*S*,3*R*)-*trans*-ACPD or **C5T** and the [(2*S*,4*S*)-4-methylglutamic acid] (**4T**)³⁷ activated the metabotropic subtype group I, while **C5T** and (2*S*,3*S*,4*S*)-L-CCG-I activated the group II of metabotropic receptor.^{13,14}

On the basis of the physical features known for specific metabotropic (group I and group II) and specific ionotropic (NMDA and KA) agonists, respectively, it was possible to

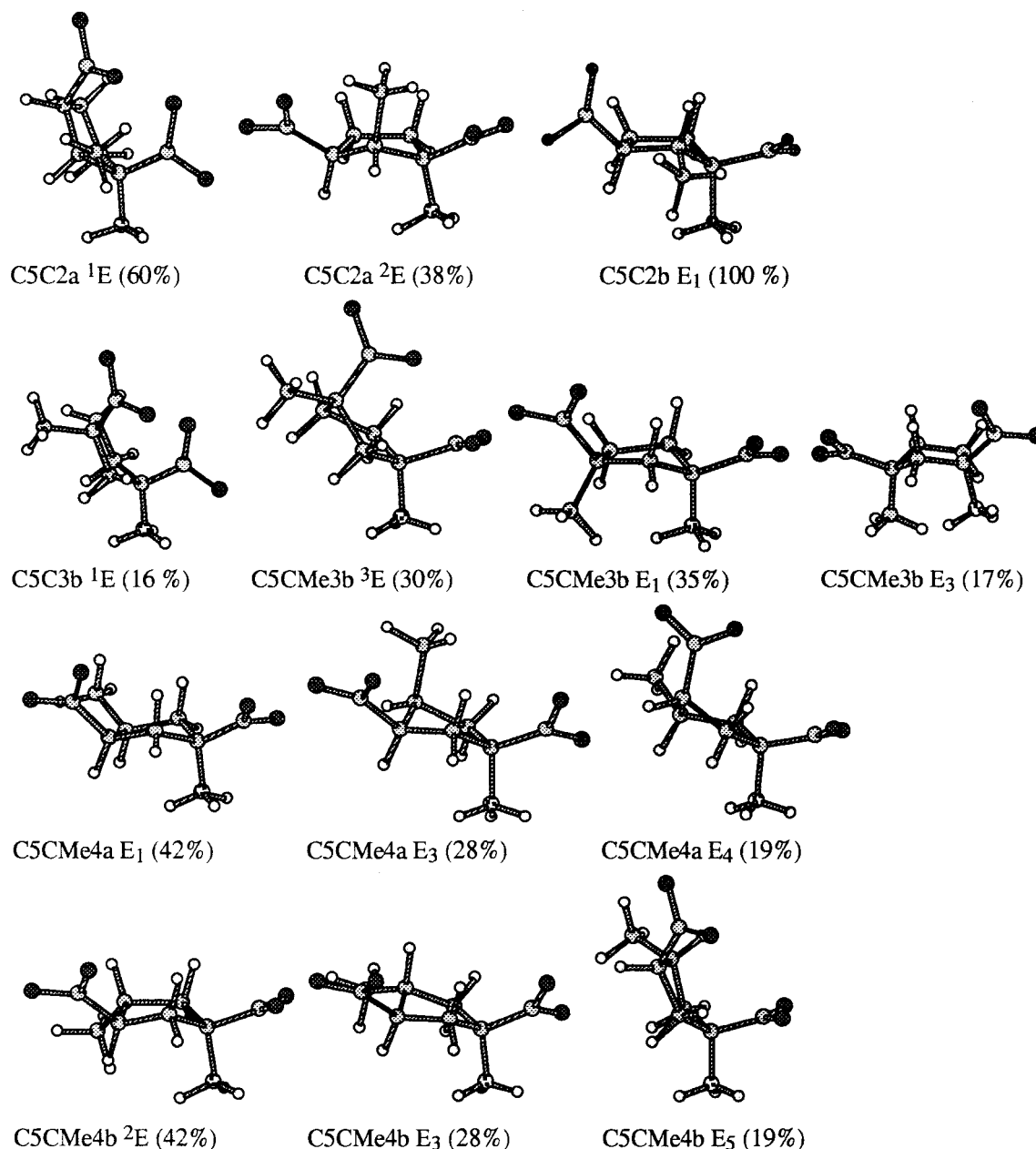


Figure 8. Achieved conformations for the methyl-*cis*-C5 molecules by MD and only the forms, *envelope E* are represented; potential energies of the corresponding C5 molecules.

extract a binding glutamate conformation to a subtype receptor (Figure 10) in light of the conformational preferences in solution of each of the studied compounds.

(A) Structural Characteristics of the Methylated-ACPD. The different envelopes are grouped into the different classes (F_I – F_{IV}) previously described (Table 7, Figures 2 and 3). The methyl-ACPD, substituted by a methyl at the C(2), C(3), and C(4) carbons, can be compared to the two cyclic ACPD compounds according to their major conformations existing in solution and to their biological activities.

In all of the compounds, the ring closure does not allow a negative *gauche*- g^- value for the torsion angle (χ_1), such as g^- -C and also g^- -c (χ_2) for all of the *trans*-ACPD isomers. The *cis*-ACPD belongs to the families F_{II} (Aa), F_{III} (Ba), and F_{IV} (Bc), while the families F_I (Ab), F_{II} (Aa), and F_{III} (Ba) represent the *trans*-ACPD. The conformations tg^- -Ac,

g^-g^- -Cc (F_I), g^-t -Ca (F_{III}) and g^-t -Cb (F_{IV}) are totally forbidden in all the cyclic ACPD compounds.

In Figures 11 and 12, we have represented the major conformations of the different compounds according to the family classes. We can observe that the conformational averaging (Figures 7–9) of **C5C4b** (83% F_{II} , 3% F_{III} , and 14% F_{IV}) and **C5T4b** (58% F_I , 17% F_{II} , and 25% F_{III}) are similar to those of **C5C** (84% F_{II} and 16% F_{IV}) and **C5T** (47% F_I , 17% F_{II} , and 36% F_{III}), respectively. Thus, the structural change in the derivatives substituted in position **4b** by a methyl group does not induce any conformational differences, and it would not be expected to profoundly affect their biological properties.

In all of the other methylated-ACPD molecules, the presence of the methyl in a particular position on the cyclic ACPD backbone led to a restricted number of conformations. This extensive conformational investigation has clearly

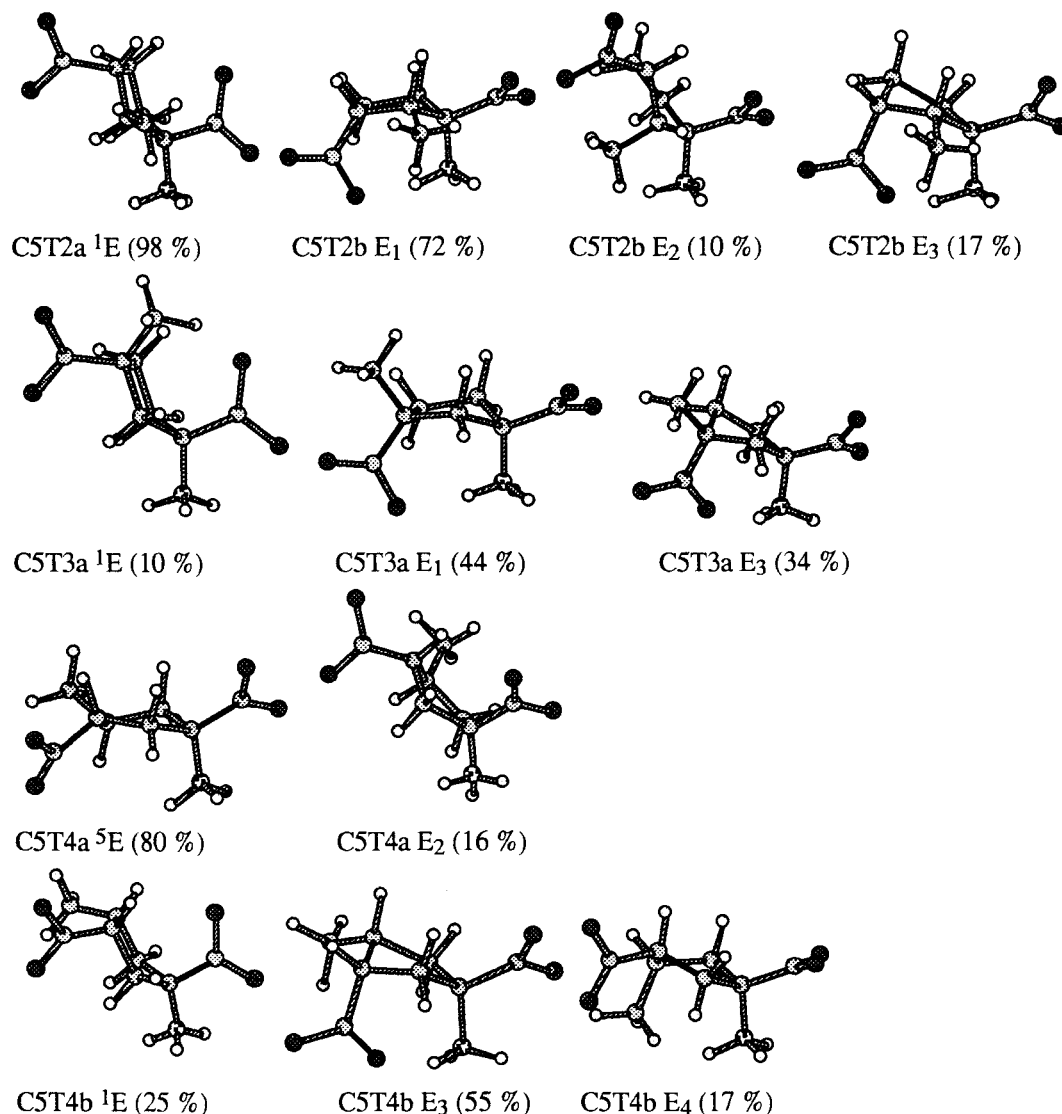


Figure 9. Achieved conformations for the methyl-*trans*-C5 molecules by MD and only the forms, *envelope E* are represented; potential energies of the corresponding C5 molecules.

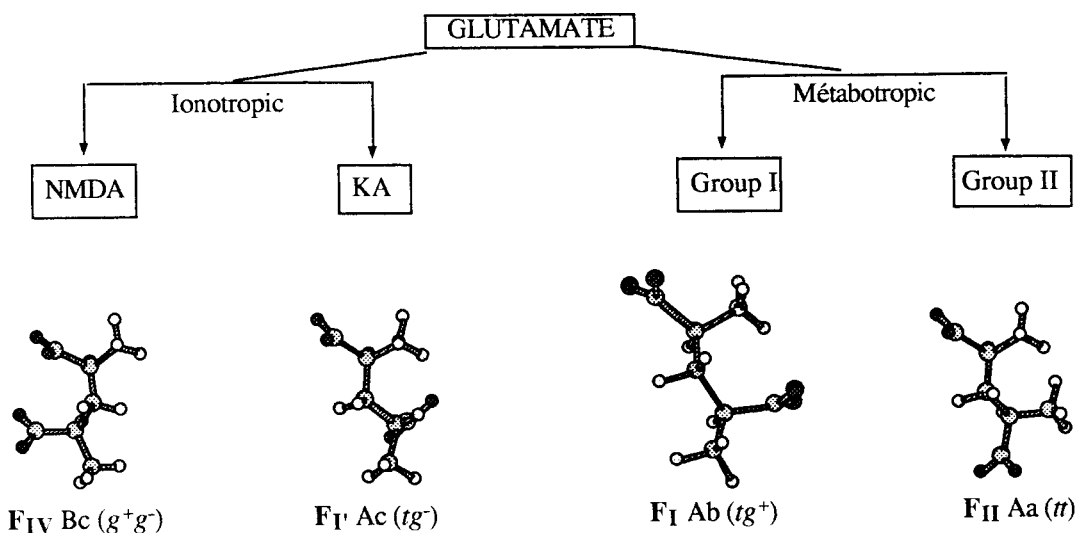


Figure 10. Representation of the different conformational families I, I', II, and IV of glutamic acid corresponding to Ab, Ac, Aa, and Bc, respectively, which activate different glutamate receptors.

established the privileged conformation of each methylated-ACPD analogue such as C5C2a (62% F_{IV}) and C5C2b

(100% F_{II}), C5C3b (50% F_{II} and F_{IV}), C5C4a (72% F_{II}) and C5C4b (83% F_{II}), C5T2a (100% F_{III}) and C5T2b (90%

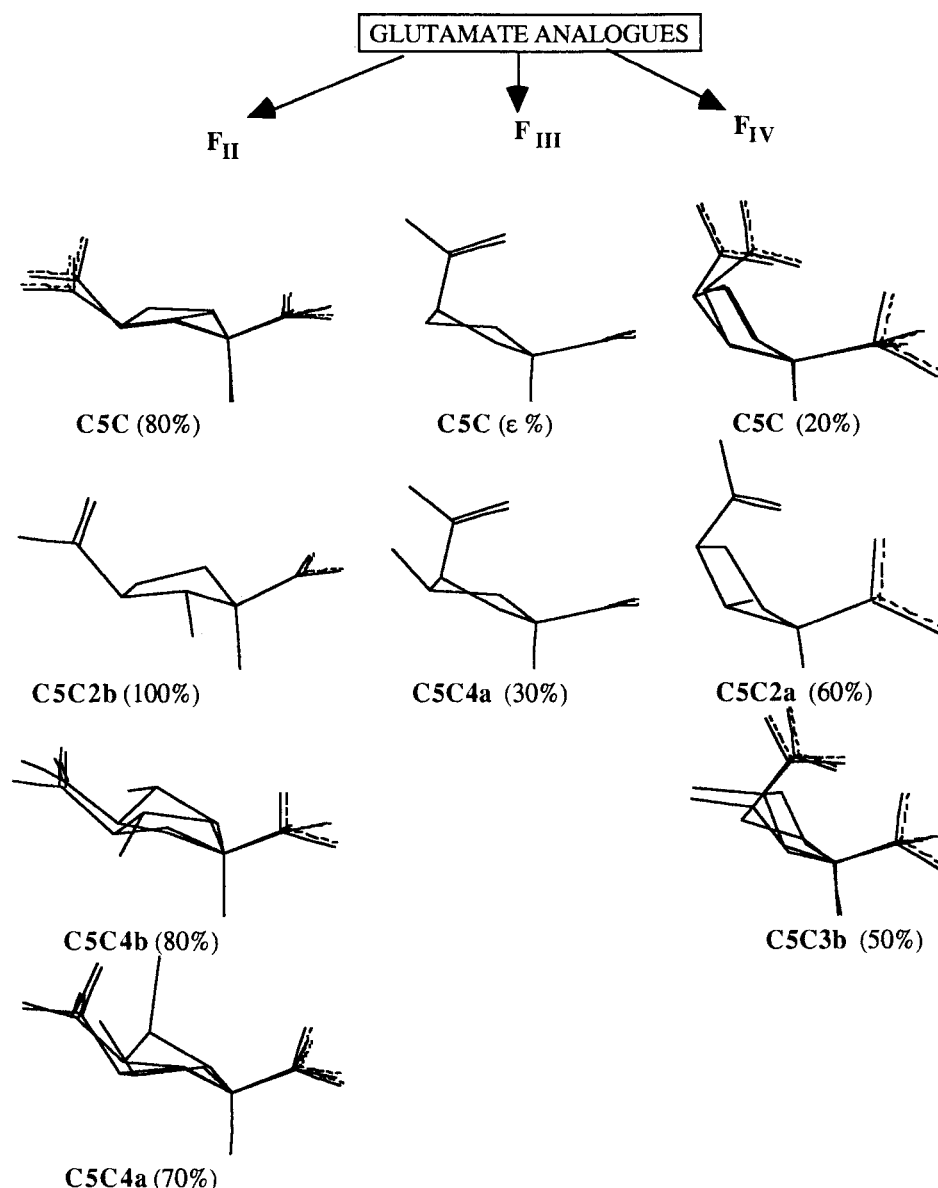


Figure 11. Representation of the different conformational families **F_{II}**, **F_I**, and **F_{IV}** corresponding to **C5C2a**, **C5C2b**, **C5C3b**, **C5C4a**, and **C5C4b** for the **C5C** isomer.

F_I), **C5T3a** (80% **F_I**), **C5T4a** (80% **F_{II}**), and **C5T4a** (58% **F_I**) (Figure 12). Thus, according to their biological results, it will be possible to establish the major glutamate conformation of specific inducers of glutamate receptors as it seems difficult to reach a particular high free energy conformation adopted by the molecule after binding to the receptor, if the different groups potentially active in the binding site (α -CO₂⁻, α -NH₃⁺, and γ -CO₂⁻) do not present beforehand a particular spatial topology.

(B) Structural Characteristics of Specific Metabotropic (Groups I–II) Ligands. The metabotropic glutamate receptors (mGluRs) are characterized by eight mGluRs^{10,12} which are classified into three groups of which group I and group II are activated by (1*S*,3*R*)-*trans*-ACPD.^{12–14}

trans-ACPD (**C5T**) adopts multiple conformations (A, B, a, b) of glutamate's backbone embedded in this cyclic analogue. In this agonist, the C(2)–C(3) and C(3)–C(4) rotors cannot adopt a *g*⁻-C and *g*⁻-c conformation, respectively. This metabotropic agonist belongs to the conformational families **F_I**–**F_{III}**, and these three families may be in

qualitative agreement with the active form (47% **F_I**, 17% **F_{II}**, and 36% **F_{III}**).

(1) Group I. Group I is activated by **C5T** and **4T**. The **4T** compound has been tested on the group I metabotropic receptor, and it exhibited an activity similar to glutamate. The analogue **4T** belongs mainly to the **F_I** family (60%) with the conformer *tg*⁺-Ab. The 4-methylglutamate **4T** showed a remarkable substituent effect on the increased energy difference between the global minimum energy Ab and other conformations. This allows us to conclude that high rotational barriers have to be passed for the **4T** isomer to obtain the different conformations which participate in the solution. An energy gap of 3.5–12.3 kcal mol⁻¹ could be evaluated between **4T** *tg*⁺-Ab and the values obtained for the other conformers. Clearly, the **4T** Ab conformation appears to be particularly stable. The electrostatic interaction between the α -NH₃⁺ and the γ -CO₂⁻ groups stabilized the Ab conformation and so the **F_I** Family.

Thus, the binding conformations of the metabotropic receptors correspond to the conformations *t*-A, *g*⁺-B and *t*-a,

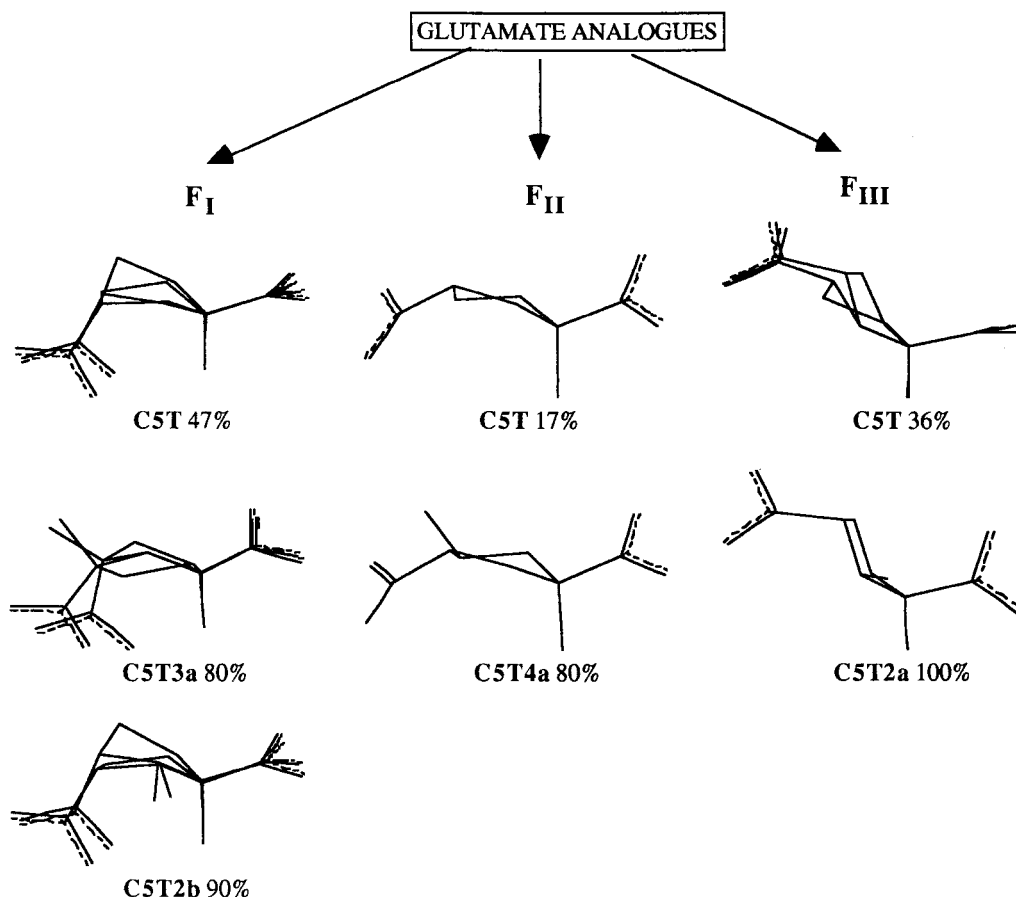


Figure 12. Representation of the different conformational families **F_I**, **F_{II}**, and **F_{III}** corresponding to **C5T2a**, **C5T2b**, **C5T3a**, and **C5T4a** for the **C5T** isomer.

g^+-b (Figure 1) relative to the C(2)–C(3) and C(3)–C(4) torsion angles, respectively.²⁰ In particular, the **F_I** family (the two *t*-A and g^+-b rotamers) seems essential for the interaction at the group I receptor,¹⁹ and it is finding predominance in **C5T2b** (90% **F_I**) and **C5T3a** (80% **F_I**).

(2) Group II. The group II metabotropic receptor is activated by (1*S*,3*R*)-*trans*-ACPD and (2*S*,3*S*,4*S*)-L-CCG-I.^{12–14} The analogue L-CCG-I belongs mainly to the **F_{II}** family. Its major Aa conformer (75%) appears to be particularly stable and adopts an “extended” conformation. The results obtained for L-CCG-I and *trans*-ACPD agonists which both exhibited a group II activity show that the *tt*-Aa conformation of glutamate embedded in these two cyclic metabotropic agonists is an important factor for the group II sub type metabotropic receptor.

Thus, the binding conformations of the metabotropic receptors are confirmed to be conformations *t*-A, g^+-B and *t*-a, g^+-b relative to the C(2)–C(3) and C(3)–C(4) torsion angle, respectively.²⁰ In particular, the **F_{II}** family (the *t*-A and *t*-a rotamers) seems to activate the group II metabotropic receptor and constitutes the major structural family of the **C5T4a** (80% **F_{II}**) isomer.

(C) Structural Characteristics of Specific Ionotropic (NMDA) Ligands. It is well-known that (1*R*,3*R*)-*cis*-ACPD was shown to be an effective agonist of NMDA receptors.^{38,39} *cis*-ACPD adopts multiple conformations (A, B, a, c) of glutamate’s C(2)–C(3) and C(3)–C(4) bonds, and it belongs to the conformational families **F_{II}** and **F_{IV}** (84% **F_{II}** and 16% **F_{IV}**). At physiological pH, both carboxyl groups are found to be in an extended position, *tt*-Aa (**F_{II}**) to reduce the steric

energy. At isoelectric pH when the 3-carboxylate group is protonated, *cis*-ACPD is represented by new privileged conformations, g^+g^- -Bc (**F_{IV}**) in which the 1-carboxylate group (1-CO₂[−]) is stabilized by an electrostatic interaction with the folded 3-carboxyl group (3-CO₂H).

The (2*S*)4-methylene-glutamic acid **4M** isomer presents a potent activity at the ionotropic glutamate receptors (NMDA).³⁶ For this compound, the conformational solution is represented by 60% of the g^+g^- -Bc conformation (**F_{IV}**). The ionotropic (NMDA) subclass of glutamate receptors is also characterized by the binding of (2*S*,3*R*,4*S*)-CCG (**L-CCG-IV**) which contains an embedded L-glutamate moiety in a partially restricted conformation (relative to the C(3)–C(4) bond). The analogue **L-CCG-IV** belongs mainly to the Bc (**F_{IV}**) conformer (45%) at pH 7.

Since the *cis*-ACPD, the **4M** isomer, and the **L-CCG-IV** isomer were found to preferentially activate NMDA receptors, the superimposition of the three characteristic functional atoms α -N, α -C, γ -C of the conformations of the three NMDA agonists has provided clear evidence that the conformation; g^+g^- -Bc (**F_{IV}**) would be the most plausible conformation of glutamate required for binding to NMDA receptors.

The binding families **F_I** and **F_{IV}** of the ionotropic receptor correspond to the conformations *t*-A, g^+-B and *t*-a, g^+-c relative to the C(2)–C(3) and C(3)–C(4) torsion angles, respectively. **F_I** and **F_{IV}** represent the active forms with a selectivity for the two receptor subtypes as NMDA and KA receptors (Figure 10).²⁰ Whereas the **F_I** family (*t*-A, g^+-c) activates KA receptors but is totally forbidden in all of the

cyclic ACPD, the **F_{IV}** family (g^+ -B, g^- -c) activates NMDA receptors (**F_{IV}**). This major structure appears to be particularly stable for **C5C2a** (60% **F_{IV}**) and **C5C3b** (50% **F_{IV}**) which adopt this "folded" conformation.

CONCLUSION

This work has provided determination of new ligand structures, and the results underline the specificity of the influence of electrostatic and steric interactions for each compound. The conformation depends strongly on carbon substitution and on the geometrical isomerism of the methyl. This aspect makes methyl-*cis*-ACPD and methyl-*trans*-ACPD interesting tools for studies of conformational preferences of glutamate subtype receptors. We can suppose that the presence of this additional methyl group would not cause a major steric exclusion effect to the binding site.

This study was of great benefit in predicting the specific range of conformations available to each derivative in solution. The resulting conformations of methyl-*cis*-ACPD and methyl-*trans*-ACPD have been elucidated by a conformational analysis using a combination of mechanics and dynamics calculations. Beforehand, it has been necessary to develop a conformational analysis of the native molecules (*cis*- and *trans*-ACPD) using a combination of NMR experimental results, mechanics and dynamics calculations, and theoretical simulation of NMR spectra and to fit molecular modeling and experimental NMR data to apply the same parameters in the CVFF force field for modeling the methylated derivatives.

This predictive MD study shall provide the basis for further NMR studies of the methyl-ACPDs analogues. The final structures obtained from this MD study will be afterward compared with the conformations derived from NMR data, and the conformations of cyclopentane ring will be elucidated from a knowledge of all the theoretical vicinal coupling constants.

The MD study led to a number of "extended" (**F_{II}**, **F_{III}**) or "folded" forms (**F_I**, **F_{IV}**) in very satisfactory agreement with an expected selectivity since a particular glutamate receptor is privileged for each isomer considered. The conformational preferences of methyl-*cis*-ACPD and methyl-*trans*-ACPD are discussed in light of the physical features known for specific metabotropic agonists (group I and II) and specific ionotropic agonists (NMDA), respectively.

From these preliminary results, the synthesis and pharmacological activities of these new conformationally constrained cyclic analogues of glutamic acid will be attempted in a next step, according to the requested agonist: **F_I** (**C5T2b**, 90%; **C5T3a**, 80%; **C5T4b**, 60%), **F_{II}** (**C5C2b**, 100%; **C5C4b**, 80%; **C5T4a**, 80%; **C5C4a**, 70%), **F_{III}** (**C5T2a**, 100%), or **F_{IV}** (**C5C2a**, 60%; **C5C3b**, 50%).

MATERIALS AND METHODS

Nuclear Magnetic Resonance. All NMR spectra were recorded on a Bruker AMX-500 spectrometer on samples dissolved in deuterium oxide. At pH 7, the samples were dissolved in an aqueous NaD₂PO₄-Na₂DPO₄ buffer, and it was possible to attain concentrations of 0.04 mol dm⁻³ for ¹H and 0.14 mol dm⁻³ for ¹³C experiments. The coupling constants are given with a precision of 0.3 Hz. The spectrum

simulation was carried out on a Macintosh II computer using the software NMR II.

The 2D ¹H, ¹H COSY spectra were acquired by recording 128 free induction decay (FIDs) of 512 points. The relaxation delay was set to 3.5 s. The spectral width was set to 1500 Hz for proton spectra and 31250 Hz for carbon spectra. The 90° pulse was 5.7 μs, the relaxation delay was 1 s, and each FID was acquired with 64 scans. The data were zero-filled, and the final size of the matrices was 2 × 1 K to 1024 and 512 points in *f*₂ and *f*₁, respectively, prior to double Fourier transformations with an unshifted sine-bell window function in both dimensions. Inverse correlation HMQC experiments⁴⁰ were recorded using a transfer delay (¹/₂*J*_{C-H}) of 3.33 ms.

The 2D *J* δ selective INEPT²⁴ experiment using polarization transfer from ¹H to ¹³C gave long-range heteronuclear coupling constants ³*J*_{¹³C-¹H}. The selective excitation of a proton signal allows detection of a single doublet for the corresponding coupled carbon(s). At 500 MHz, selectivity was achieved by a DANTE-type pulse train generated by the decoupler channel. This experiment was carried out at 300 K with 256 scans of 4K data points, 64 experiments, a spectral width of 220 ppm in *f*₂, and 0.125 ppm in *f*₁.

Computer Simulations. The conformations of these compounds that were incorporated into the analysis were initially built from X-ray crystal data of **C5T**. Charges and atomic potentials were then redefined for the new molecules using the built-in algorithm of the BIOSYM molecular modeling software on a Silicon Graphics workstation.

Energy minimization and MD simulations were performed using the consistent valence force field (CVFF) from Dauber-Osguthorpe et al.²⁸ Charges and atomic potentials come from the BIOSYM residue library are derived by empirical fitting, that is, adjusting the potential parameters and charges until they can reproduce the crystal structure. To mimic ionization at neutral pH, an sp³+ hybridization was assigned to the amine, increasing the molecular electrostatic total charge by + 1.

To mimic the solvent effect, the relative permittivity was set to be distance-dependent, $\epsilon = R_{ij}$ ($\epsilon = 5$, $\epsilon = 4r$)³¹ in the description of the Coulombic interaction. Another protocol was used with explicit solvent molecules incorporated during the run. With Biosym software a procedure was selected using a cube of volume 12 × 12 × 12 Å³ containing 48 water molecules to allow periodic boundary conditions and a nonbonded cutoff distance of 11 Å. The relative permittivity was set to $\epsilon = 1$. In these cases, the energies to be compared are those of "molecule + *x*H₂O" systems in various situations.

The first step in the modeling consisted of minimizing the structure previously constructed, "steepest descent" and "conjugate gradients" methods, until convergence.

The second step of the conformational sampling procedure consisted of recording MD trajectories (including the charge distributions in CVFF force field). Molecular conformers were sampled during a 200 ps MD trajectory at 300 K (or 100 ps with 48 water molecules). A time step of 1 fs was used, and the system was equilibrated for 6 ps. A conformation was stored each picosecond so that 200 conformations (or 100 with 48 water molecules) were recorded by the end of the MD simulation. For a preliminary exploration of the conformational space, after energy minimization and an

equilibration period of 6 ps, we performed a 50 ps MD run at 300 K with periodic temperature jumps to 600 K to supply the system with energy (to pass conformational barriers). The 50 ps trajectory is sampled every picosecond, and the remaining structures are then minimized by molecular mechanics and stored. The final conformers found with lowest energies were then further minimized to a gradient less than 0.01 kcal mol⁻¹ to obtain their energies at higher accuracy.

The sampling every picosecond was believed to be a sufficiently long time for an atom with significant movement and sufficiently short for a correct sampling of the conformational space.

All molecular conformations were compared using the analysis module of the software. Conformational similarities were evaluated by calculating the root mean square of deviation between heavy atoms for each possible pair of the different structures. The results represent group of structures whose small root mean square deviations (<0.5 Å) suggested that they may belong to the same conformational family. Conformational representatives extracted from each family were compared for each compound, as well as between different ligands, using a superimposition procedure.

REFERENCES AND NOTES

- (1) Watkins, J. C.; Evans, R. H. Excitatory amino acid transmitters. *Annu. Rev. Pharmacol. Toxicol.* **1981**, *21*, 165–204.
- (2) Davies, J.; Evans, R. H.; Francis, A. A.; Jones, A. W.; Smith, D. A. S.; Watkins, J. C. Conformational aspects of the actions of some piperidine dicarboxylic acids at excitatory amino acid receptors in the mammalian and amphibian spinal cord. *Neurochem. Res.* **1982**, *7*, 1119–1133.
- (3) Bliss, T. V. P.; Collingridge, G. L. A synaptic model of memory: Long term potentiation in the hippocampus. *Nature* **1993**, *361*, 31–39.
- (4) Choi, D. W. Glutamate Neurotoxicity and Diseases of the Nervous System. *Neuron* **1988**, *1*, 623–643.
- (5) Pin, J. P.; Duvoisin, R. The Metabotropic Glutamate Receptors: Structure and Functions. *Neuropharmacology* **1995**, *34*, 1–26.
- (6) Schoepp, D. D.; Conn, P. J. Metabotropic glutamate receptors in brain function and pathology. *Trends Pharmacol. Sci.* **1993**, *14*, 13–20.
- (7) Nakanishi, S. Molecular diversity of glutamate receptors and implications for brain function. *Science* **1992**, *258*, 597–603.
- (8) Sommer, B.; Seeburg, P. H. *Trends Pharmacol. Sci.* **1992**, *13*, 291–296.
- (9) Houamed, K. M.; Kuijper, J. L.; Gilbert, T. L.; Haldeman, B. A.; O'Hara, P. J.; Mulvihill, E. R.; Almers, W.; Hagen, F. S. Cloning expression and gene structure of a G-protein-coupled glutamate receptor from rat brain. *Science* **1991**, *252*, 1318–1321.
- (10) Abe, T.; Sugihara, H.; Nawa, H.; Shigemoto, R.; Mizuno, N.; Nakanishi, S. Molecular characterization of a novel metabotropic glutamate receptor mGluR5 coupled to inositol phosphate/Ca²⁺ signal transduction. *J. Biol. Chem.* **1992**, *267*, 13361–13368.
- (11) Tanabe, Y.; Masu, M.; Ishii, T.; Shigemoto, R.; Nakanishi, S. A family of metabotropic glutamate receptors. *Neuron* **1992**, *8*, 169–172.
- (12) Tanabe, Y.; Nomura, A.; Masu, M.; Shigemoto, R.; Mizuno, N.; Nakanishi, S. Signal transduction, pharmacological properties and expression patterns of two rat metabotropic glutamate receptors, mGluR3 and mGluR4. *J. Neurosci.* **1993**, *13*, 1372–1378.
- (13) Ishida, M.; Saitoh, T.; Shinozaki, H. A new metabotropic glutamate receptor agonist: Developmental change of its sensitivity to receptors in the newborn rat spinal cord. *Neurosci. Lett.* **1993**, *160*, 156–158.
- (14) Ohfun, Y.; Shinozaki, H. In *L-2-(carboxycyclopropyl)glycines. Conformationally constrained L-glutamate analogues*; Kozikowski, A. P., Ed.; Raven Press, Ltd.: New York 1993.
- (15) Okamoto, N.; Hori, S.; Akazawa, C.; Hayashi, Y.; Shigemoto, R.; Mizuno, N.; Nakanishi, S. Molecular characterization of a new metabotropic glutamate receptor mGluR7 coupled to inhibitory cyclic AMP signal transduction. *J. Biol. Chem.* **1994**, *269*, 1231–1236.
- (16) O'Hara, P. J.; Sheppard, P. O.; Thøgersen, M.; Venezia, D.; Haldeman, B. A.; Mc Crane, V.; Houamed, K. M.; Thomsen, C.; Gilbert, T. L.; Mulvihill, E. R. The ligand-binding domain in metabotropic glutamate receptors is related to bacterial periplasmic binding proteins. *Neuron* **1993**, *11*, 41–52.
- (17) Chamberlin, R.; Bridges, R. In *Conformational constrained acidic amino acids as probes of glutamate receptors and transporters*; Kozikowski, A., Ed.; Raven Press: New York, 1993; Vol. 9, pp 231–259.
- (18) Larue, V.; Gharbi-Benarous, J.; Acher, F.; Valle, G.; Crisma, M.; Toniolo, C.; Azerad, R.; Girault, J. P. Conformational Analysis by NMR Spectroscopy, Molecular Dynamics Simulation in Water and X-Ray Crystallography of Glutamic Acid Analogues: Isomers of 1-Amino-1,3 Cyclopentane Dicarboxylic Acid (ACPD). *J. Chem. Soc., Perkin Trans. 2* **1995**, 1111–1126.
- (19) Todeschi, N.; Gharbi-Benarous, J.; Acher, F.; Azerad, R.; Girault, J. P. Conformational analysis by NMR spectroscopy and molecular simulation in water of methylated glutamic acids, agonists at glutamate receptors. *J. Chem. Soc., Perkin Trans. 2* **1996**, 1337–1351.
- (20) Todeschi, N.; Gharbi-Benarous, J.; Acher, F.; Larue, V.; Pin, J. P.; Bockaert, J.; Azerad, R.; Girault, J. P. Conformational Analysis of Glutamic Acid Analogues as Probes of Glutamate Receptors using Molecular Modeling and NMR methods. Comparison with Specific Agonists. *Bioorg. Med. Chem.* **1997**, *5*, 335–352.
- (21) Todeschi, N.; Gharbi-Benarous, J.; Arulmozhi, V.; Acher, F.; Azerad, R.; Girault, J. P. Conformational Study in Water by NMR and Molecular Modeling of α -Methyl α -Amino Acid: Differential Conformational Properties of α -Cyclic and α -Methylglutamic Acid. *J. Chem. Inf. Comput. Sci.*, in press.
- (22) Todeschi, N.; Gharbi-Benarous, J.; Girault, J. P. Structure of Kainic Acid Totally Elucidated by NMR and Molecular Modeling. *Bioorg. Med. Chem.* **1997**, *5*, 1943–1957.
- (23) Evrard-Todeschi, N.; Gharbi-Benarous, J.; Cosse-Barbi, A.; Thiroit, G.; Girault, J.-P. Conformational Analysis of 2-(Carboxy-Cyclopropyl) Glycines Agonists of Glutamate Receptors in Aqueous Solution using a combination of NMR and Molecular Modelling Experiments and charges calculations. *J. Chem. Soc., Perkin Trans 2* **1997**, 2677–2689.
- (24) Ladam, P.; Gharbi-Benarous, J.; Pioto, M.; Delaforge, M.; Girault, J. P. Determination of Long-Range ¹³C-¹H Coupling Constants of Macrolide Antibiotics by 2D J- δ Selective INEPT Experiments. *Magn. Reson. Chem.* **1994**, *32*, 1–7.
- (25) Altona, C.; Sundaralingam, M. Conformational Analysis of the Sugar Ring in Nucleosides and Nucleotides. Improved Methods for the Interpretation of Proton Magnetic Resonance Coupling Constants. *J. Am. Chem. Soc.* **1973**, *95*, 2333–2344.
- (26) Haasnoot, C. A. G.; De Leeuw, F. A. A. M.; Altona, C. The relation between proton-proton NMR coupling constants and substituent electronegativities. I. An empirical generalization of the Karplus equation. *Tetrahedron* **1980**, *36*, 2783–2792.
- (27) Tvaroska, I.; Hricovini, M.; Petrakova, E. An attempt to derive a new Karplus-type equation of vicinal proton-carbon coupling constants for C-O-C-H segments of bonded atoms. *Carbohydr. Res.* **1989**, *189*, 359–362.
- (28) Dauber-Osguthorpe, P.; Roberts, V. A.; Osguthorpe, D. J.; Wolff, J.; Genest, M.; Hagler, A. T. Structure and Energetics of Ligand Binding to Proteins: E. coli Dihydrofolate Reductase-Trimethoprim, A Drug-Receptor System. *Proteins: Struct. Funct., Gene* **1988**, *4*, 31–47.
- (29) Clark, M.; Cramer, R. D.; Van Opdenbosh, N. *J. Comput. Chem.* **1989**, *10*, 982–1012.
- (30) Burt, S. K.; Mackay, D.; Nagler, A. T. In *Computer-Aided Drug Design*; Perun, T. J., Propst, C. L., Eds.; Marcel Dekker and Basel: New York, 1989; p 66.
- (31) Morelle, N.; Gharbi-Benarous, J.; Acher, F.; Valle, G.; Crisma, M.; Toniolo, C.; Azerad, R.; Girault, J. P. Conformational analysis of cyclohexane-derived analogues of glutamic acid by X-ray crystallography, NMR spectroscopy in solution and molecular dynamics. *J. Chem. Soc., Perkin Trans. 2* **1993**, 525–533.
- (32) van Gunsteren, W. F.; Berendsen, H. J. C. Computer Simulation of Molecular Dynamics: Methodology, Applications, and Perspectives in Chemistry. *Angew. Chem., Int. Ed. Engl.* **1990**, *29*, 992–1023.
- (33) Kessler, H.; Griesinger, C.; Lautz, J.; Müller, A.; van Gunsteren, W. F.; Berendsen, H. J. C. Conformational Dynamics Detected by Nuclear Magnetic Resonance NOE values and J Coupling Constants. *J. Am. Chem. Soc.* **1988**, *110*, 3393–3396.
- (34) Hünenberger, P. H.; Mark, A. E.; van Gunsteren, W. F. Fluctuation and cross-correlation analysis of protein motions observed in nanosecond molecular dynamics simulations. *J. Mol. Biol.* **1995**, *252*, 492–503.
- (35) Querfelli, O.; Ishida, M.; Shinozaki, H.; Nakanishi, K.; Ohfun, Y. Efficient Synthesis of 4-Methylene-L-glutamic Acid and its Analogues. *Synlett* **1993**, 409–410.

- (36) Gu, Z. Q.; Hesson, D.; Pelletier, J. C.; Meccecchini, M. L. Synthesis, Resolution and Biological Evaluation of the Four Stereoisomers of 4-Methylglutamic Acid: Selective Probes of Kainate Receptors. *J. Med. Chem.* **1995**, *38*, 2518–2520.
- (37) Pin, J. P.; Waeber, C.; Prézeau, L.; Bockaert, J.; Heinemann, S. F. Alternative splicing generates metabotropic glutamate receptors inducing different patterns of calcium release in *Xenopus* oocytes. *Proc. Natl. Acad. Sci. U.S.A.* **1992**, *89*, 10331–10335.
- (38) Curry, K.; Peet, M. J.; Magnuson, D. S. K.; McLennan, H. Synthesis, Resolution, and Absolute Configuration of the Isomers of the Neuronal Excitant 1-Amino-1,3-cyclopentanedicarboxylic Acid. *J. Med. Chem.* **1988**, *31*, 864–867.
- (39) Curry, K. Rigid analogues as probes of excitatory amino acid receptors. *Can. J. Physiol. Pharmacol.* **1991**, *69*, 1076–1083.
- (40) Hurd, R. E.; John, B. K. Gradient-enhancement proton-detected heteronuclear multiple-quantum coherence spectroscopy. *J. Magic Reson.* **1991**, *91*, 648–653.

CI9802023